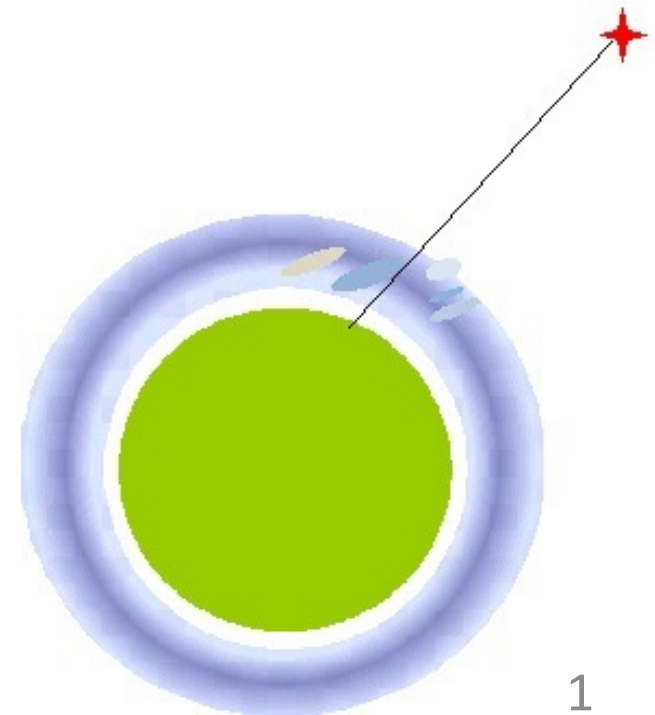


Modern status of the theory of high frequency wave propagation in the ionosphere

N.N. Zernov, V.E. Gherm, M.A. Bisyarin

St. Petersburg State University, St. Petersburg, Russia



Mathematical methods for solving the problems of the high frequency wave propagation in the transionospheric and ionospheric reflection channels.

N.N. Zernov, B. Lundborg. The Statistical Theory of Wave Propagation and HF Propagation in the Ionosphere with Local Inhomogeneities. ISSN 0284-1703. 138 pp. Swedish Institute of Space Physics, Uppsala Division, Sweden, (printed in Kiruna), 1993. – TEXTBOOK

Selected papers, referred to below, which contain the results to be discussed:

Transionospheric channel:

1. V.E. Gherm, N.N. Zernov, S.M. Radicella, H.J. Strangeways. Propagation model for signal fluctuations on transionospheric radio links. *Radio Science*, 35, 5, 1221-1232, 2000.
2. V.E. Gherm, N.N. Zernov, H.J. Strangeways. Propagation Model for Transionospheric Fluctuational Paths of Propagation: Simulator of the Transionospheric Channel. *Radio Science*, 40(1), RS1003, doi: 10.1029/2004RS003097, 2005.
3. Maurits, S.A., V.E. Gherm, N.N. Zernov, and H.J. Strangeways (2008), Modeling of scintillation effects on high-latitude transionospheric paths using ionospheric model (UAF EPPIM) for background electron density specifications, *Radio Science*, 43, RS4001, doi:10.1029/2006RS003539.
4. Zernov, N.N., V.E. Gherm, and H.J. Strangeways (2009), On the effects of scintillation of low-latitude bubbles on transionospheric paths of propagation, *Radio Science*, 44, RS0A14, doi:10.1029/2008RS004074.

5. Gherm, V.E., N.N. Zernov, and H.J. Strangeways, (2011), Effects of diffraction by ionospheric electron density irregularities on the range error in GNSS dual-frequency positioning and phase decorrelation, *Radio Science*, 46, RS3002, doi:10.1029/2010RS004624.
6. Zernov, N.N., V.E. Gherm, and H.J. Strangeways, (2012), Further determinations of strong scintillation effects on GNSS signals using the Hybrid Scintillation Propagation Model, *Radio Science*, 47, RS0L06, 2011RS004935R. doi:10.1029/2011RS004935.
7. Strangeways, H.J., N.N. Zernov, and V.E. Gherm, (2014), Comparison of four methods for transionospheric scintillation evaluation, *Radio Science*, 49, 899–909, doi:10.1002/2014RS005408.
8. Zernov, N.N., and V.E. Gherm, (2015a), Strong Scintillation of GNSS Signals in the Inhomogeneous Ionosphere. 1: Theoretical Background, *Radio Science*, Volume 50, Issue 2, February 2015, pp. 153 – 167. February, 2015. DOI: 10.1002/2014RS005603.
9. Gherm, V.E., and N.N. Zernov, (2015b), Strong Scintillation of GNSS Signals in the Inhomogeneous Ionosphere. 2: Simulator of Transionospheric Channel, *Radio Science*, Volume 50, Issue 2, February 2015, pp. 168 – 176. February, 2015. DOI: 10.1002/2014RS005604.
10. Gherm V. E., Zernov N.N. Extension of Hybrid Scintillation Propagation Model to the case of field propagation in the ionosphere with highly anisotropic irregularities. *Radio Science*. 2017. V. 52. pp. 874-883, 2017, doi:10.1002/2017RS006264.

11. Nikolay N. Zernov, Andrei V. Driuk (2020a), Coherence properties of high-frequency wave field propagating through inhomogeneous ionosphere with anisotropic random irregularities of electron density: 1. Theoretical background, ***Journal of Atmospheric and Solar-Terrestrial Physics***, September, 2020. 205 (2020) 105313

12. Andrei V. Driuk, Nikolay N. Zernov (2020b), Coherence properties of high-frequency wave field propagating through inhomogeneous ionosphere with anisotropic random irregularities of electron density: 2. Further analysis and numerical results. ***Journal of Atmospheric and Solar-Terrestrial Physics***, September, 2020. 205 (2020) 105312

13. Mikhail A. Bisyarin, Nikolay N. Zernov (2021a). Nonlocal Markov approximation for mean field propagating in a medium with dielectric permittivity fluctuations in case of finite values of longitudinal correlation radius 1. Homogeneous background medium. ***Journal of Atmospheric and Solar-Terrestrial Physics***, 2021.
<https://doi.org/10.1016/j.jastp>. 2021.105744

14. Mikhail A. Bisyarin, Nikolay N. Zernov (2021b). Nonlocal Markov approximation for mean field propagating in a medium with dielectric permittivity fluctuations in case of finite values of longitudinal correlation radius 2. Inhomogeneous background medium. ***Journal of Atmospheric and Solar-Terrestrial Physics***, 2021.
<https://doi.org/10.1016/j.jastp>. 2021.105745

15. M. Bisyarin, V. Gherm and N. Zernov, "Extended Treatment of Statistical Moments of Random Fields in Nonlocal Markov Approximation," *2022 International Conference on Electromagnetics in Advanced Applications (ICEAA)*, 2022, pp. 061-063, doi: 10.1109/ICEAA49419.2022.9900048.

Ionospheric Reflection Channel

16. N.N. Zernov, V.E. Gherm, N.Yu. Zaalov, A.V. Nikitin. The generalization of Rytov's method to the case of inhomogeneous media and HF propagation and scattering in the ionosphere. *Radio Science*, 27, 2, 235-244, 1992.

17. N.N. Zernov, B. Lundborg. The influence of the ionospheric electron density fluctuations on HF pulse propagation. *Journal of Atmospheric and Terrestrial Physics*, 57, 1, 65-73, 1995.

18. V.E. Gherm, N.N. Zernov. Fresnel filtering in HF ionospheric reflection channel. *Radio Science*, 30, 1, 127-134, 1995.

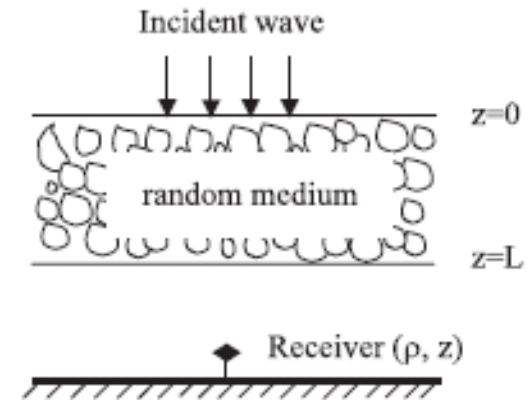
19. V.E. Gherm, N.N. Zernov, B. Lundborg, A. Vastberg. The two-frequency coherence function for the fluctuating ionosphere; narrowband pulse propagation. *Journal of Atmospheric and Solar-Terrestrial Physics*, 59, 14, 1831-1841, 1997.

20. V.E. Gherm, N.N. Zernov, B. Lundborg. The two-frequency, two-time coherence function for the fluctuating ionosphere; wideband pulse propagation. *Journal of Atmospheric and Solar-Terrestrial Physics*, 59, 14, 1843-1854, 1997.

21. V.E. Gherm, N.N. Zernov. Scattering function of the fluctuating ionosphere in the HF band. *Radio Science*, 33, 1019-1033, 1998.
22. V. Gherm, N. Zernov, B. Lundborg, M. Darnell, H. Strangeways. Wideband scattering functions for HF ionospheric propagation channels. *Journal of Atmospheric and Solar-Terrestrial Physics*, 63, 1489-1497, 2001.
23. A.A. Bitjukov, V.E. Gherm, N.N. Zernov. On the solution of Markov's parabolic equation for the second order spaced frequency and position coherence function. *Radio Science*, 37(4), RS1066, doi: 10.1029/2001RS002491, 2002.
24. A.A. Bitjukov, V.E. Gherm, N.N. Zernov. Quasi-classic approximation in Markov's parabolic equation for spaced position and frequency coherency. *Radio Science*, 38(2), 10.1029/2002RS002714, 28 March, 2003.
25. V.E. Gherm, N.N. Zernov, H.J. Strangeways. HF Propagation in a Wideband Ionospheric Fluctuating Reflection Channel: Physically Based Software Simulator of the Channel. *Radio Science*, 40(1), RS1001, doi:10.1029/2004RS003093, 2005.

Transionospheric propagation

$$S_4^2 = \frac{\langle I - \langle I \rangle \rangle^2}{\langle I \rangle^2} \quad \text{Scintillation index}$$



- Weak scintillation on the Earth's surface $S_4 < 0.6$



Complex phase method =
Rytov's method +
inhomogeneous background

- Strong scintillation on the Earth's surface $S_4 > 0.6$

- weak scintillation after passing the ionospheric layer + diffraction in the free space



Hybrid method =
complex phase method +
random screen

- strong scintillation developed inside the ionospheric layer



Markov's parabolic equations for
the field moments

INTRODUCTION

In the paper (V.E. Gherm, N.N. Zernov, S.M. Radicella, and H.J. Strangeways, “Propagation model for signal fluctuations on transionospheric radiolinks”, *Radio Science*, vol. 35, pp. 1221-1232, 2000 [1]) the initial approach was developed to study the transionospheric channel of propagation which was based on the perturbation theory to describe the field propagation between the communicating points. This approach therefore was confined by the case of weak scintillation.

The complex phase method imposed some restrictions on the range of validity of the model, which resulted in the values of the scintillation index S_4 up to 0.6, i.e. this is the case of weak scintillation.

The field strong scintillation on transionospheric paths of propagation. Propagation model 1.

To extend a propagation model to a wider range of validity (stronger scintillations), the new hybrid model was introduced which combines the complex phase method and a single random screen, properly introduced below the ionosphere (2005 [2]).

It is capable of also describing the effects of strong scintillations, e.g. focusing and saturation characterized by high values of S_4 . It can also describe some fine effects including calculation of the rate of phase changes, etc.

Propagation from a satellite to the Earth's surface is calculated in two steps:

i) spatial spectra of the field phase and amplitude are calculated by the complex phase method for the points of observation on the surface (plane or spherical) just below the ionosphere. The spectra are employed to generate a random plane or spherical screen below the ionosphere;

ii) the propagation problem for the introduced random screen is further rigorously solved to obtain the field's statistical moments and time series on the Earth's surface.

As the result, this hybrid technique allows for:

- Describing the case of strong scintillation of the field amplitude on the Earth's surface;
- Achieving the higher efficiency of numerical modelling of realistic cases of propagation as compared to the case of straightforward purely numerical multiple phase screen calculations.

The complex amplitude of the field passed through the ionosphere is represented as follows

$$E(\mathbf{r}, \omega, t) = E_0(\mathbf{r}, \omega) R(\mathbf{r}, \omega, t)$$

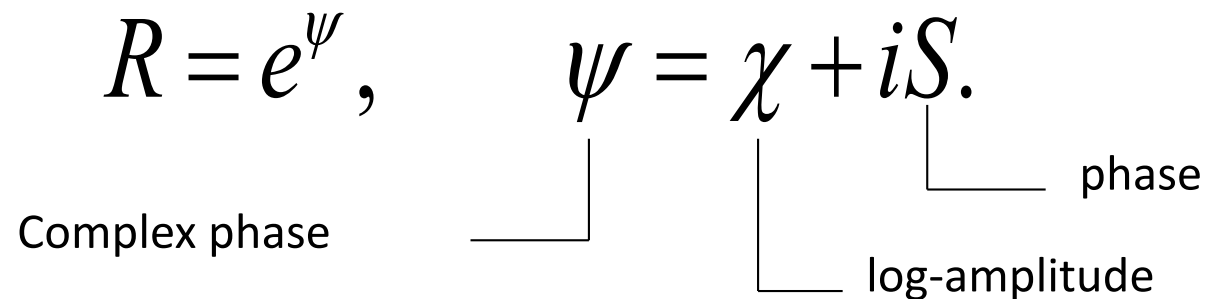
undisturbed field  random phasor

The parameter t stands for representing the slow time due to the time dependence of the electron density fluctuations.

Random phasor $R(\mathbf{r}, \omega, t)$ is treated in terms of the complex phase

$$R = e^{\psi}, \quad \psi = \chi + iS.$$

Complex phase phase
log-amplitude



To introduce a random screen just under the ionosphere, the two-dimensional spatial spectra of phase and log-amplitude are produced, which are then employed to generate the two-dimensional realisations of χ and S .

Spatial spectra of phase, log-amplitude and their cross-correlation

$$B_S(\kappa_n, \kappa_\tau) = \frac{k^2}{4} \int_0^{S_0} \frac{ds}{\varepsilon_0(s)} B_\varepsilon(0, \kappa_n, \kappa_\tau, s) \cos^2 \left\{ \frac{1}{2k} [\kappa_n^2 D_n(s) + \kappa_\tau^2 D_\tau(s)] \right\}$$

$$B_\chi(\kappa_n, \kappa_\tau) = \frac{k^2}{4} \int_0^{S_0} \frac{ds}{\varepsilon_0(s)} B_\varepsilon(0, \kappa_n, \kappa_\tau, s) \sin^2 \left\{ \frac{1}{2k} [\kappa_n^2 D_n(s) + \kappa_\tau^2 D_\tau(s)] \right\}$$

$$B_{S\chi}(\kappa_n, \kappa_\tau) = -\frac{k^2}{8} \int_0^{S_0} \frac{ds}{\varepsilon_0(s)} B_\varepsilon(0, \kappa_n, \kappa_\tau, s) \sin \left\{ \frac{1}{k} [\kappa_n^2 D_n(s) + \kappa_\tau^2 D_\tau(s)] \right\}$$

In the numerical simulation, the anisotropic inverse power law spatial spectrum of fluctuations of the ionospheric electron density is employed

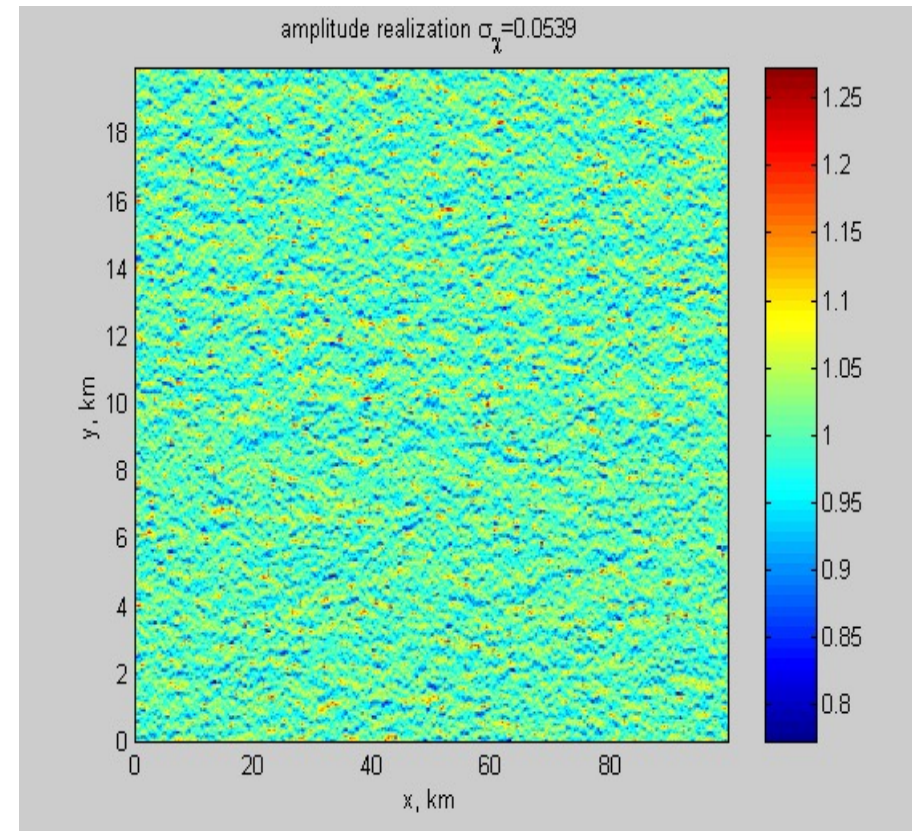
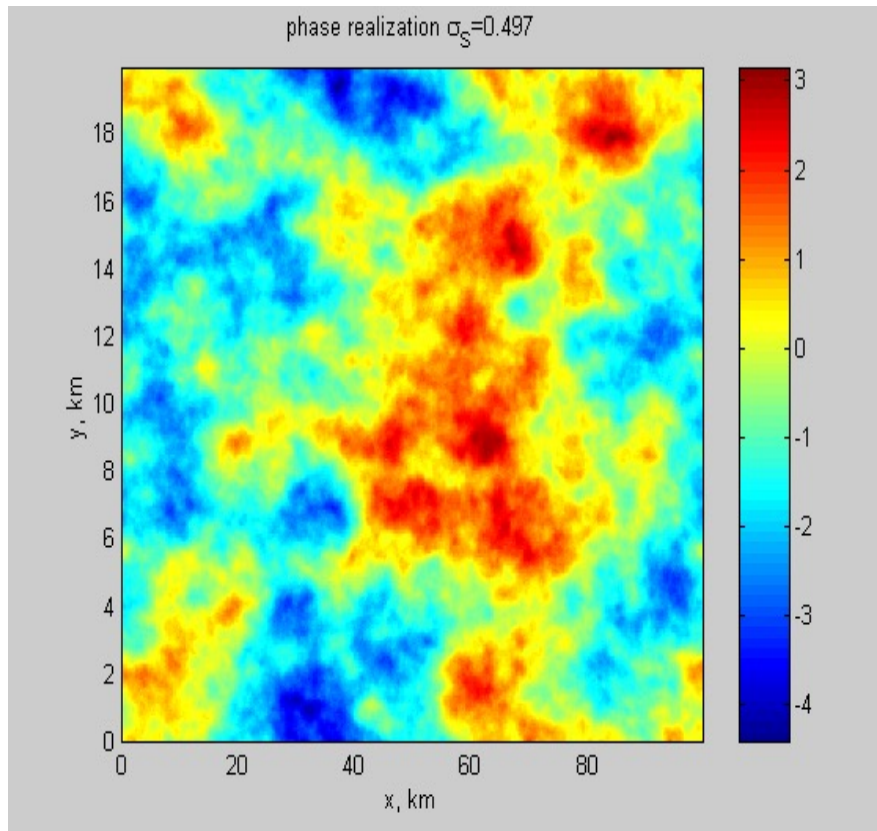
$$B_{\varepsilon}(\vec{k}, s) = C_N^2 [1 - \varepsilon_0(s)]^2 \sigma_N^2 \left(1 + \frac{K_{tg}^2}{K_{tg}^2} + \frac{\vec{K}_{tr}^2}{K_{tr}^2} \right)^{-p/2}$$

C_N^2 - normalisation coefficient

$\varepsilon_0(s)$ - distribution of the dielectric permittivity of the background ionosphere along the reference ray

σ_N^2 - variance of the fractional electron density fluctuations

Realisations of phase and amplitude on the random screen $f = 1575$ MHz



The random screen which is generated below ionosphere is not an equivalent phase screen, but the screen generated on the basis of solving the propagation problem through the fluctuating ionosphere specified by its electron density profile and a given model of fluctuation spectra.

The random complex spectrum $\tilde{E}(0, \boldsymbol{\kappa}, t)$ of the field on the screen is then transferred to the level of the Earth's surface employing the following relationship of the theory of a random screen (Fresnel propagator)

$$\tilde{E}(z, \boldsymbol{\kappa}, t) = e^{ikz} \tilde{E}(0, \boldsymbol{\kappa}, t) \exp\left(-\frac{i\boldsymbol{\kappa}^2 z}{2k}\right)$$

Examples of model outputs

Input parameters:

NeQuick profile, low-latitude ionosphere, TEC = 69 TECU.

spectral index $p=3.7$.

Variance of fluctuations $\sigma_N^2 = 10^{-2}$.

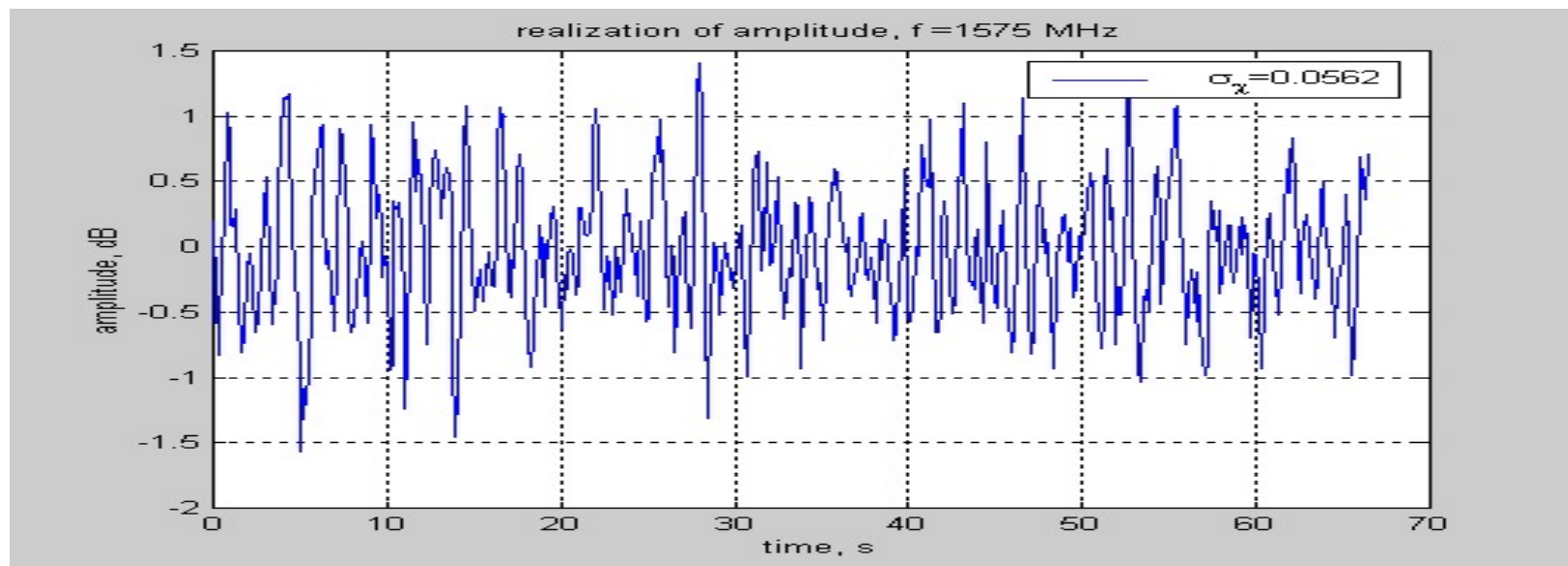
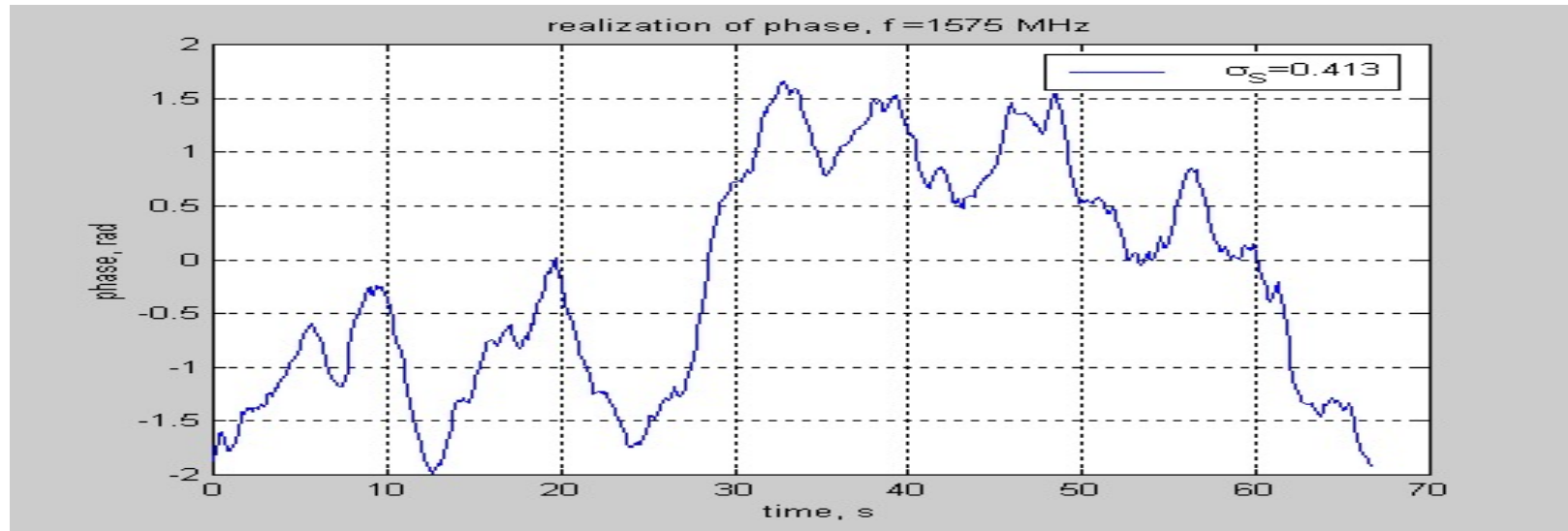
cross-field outer scale 10 km, aspect ratio $a = 5$.

Path of propagation: elevation angle of 45° , azimuth 45° .

The effective velocity of the horizontal frozen drift 300 m/s.

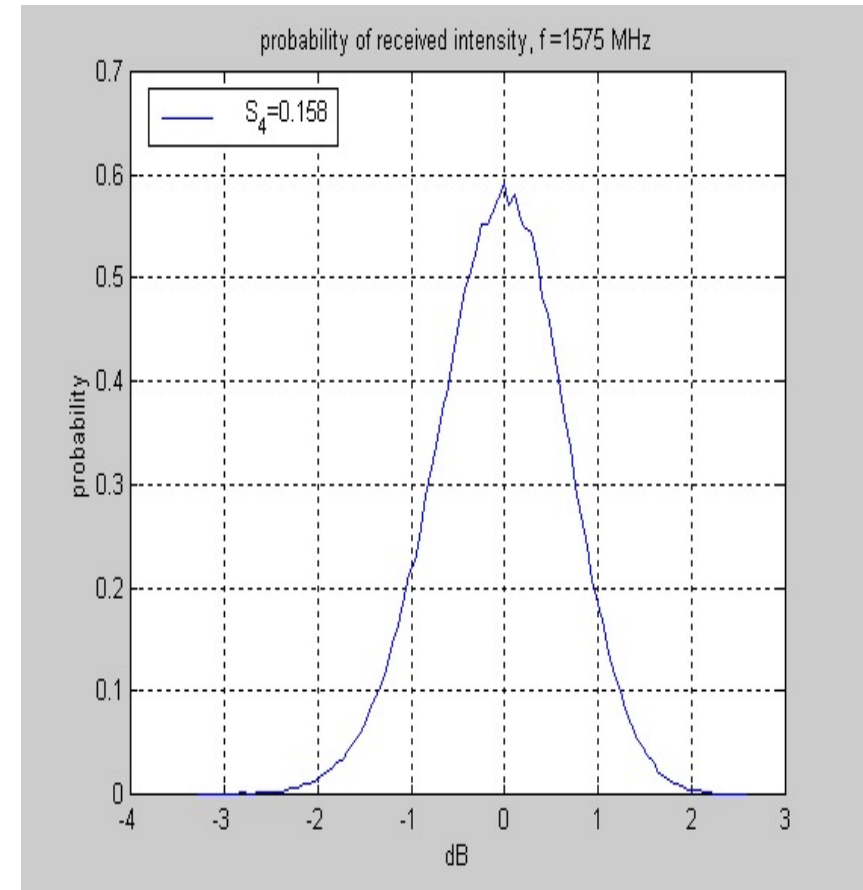
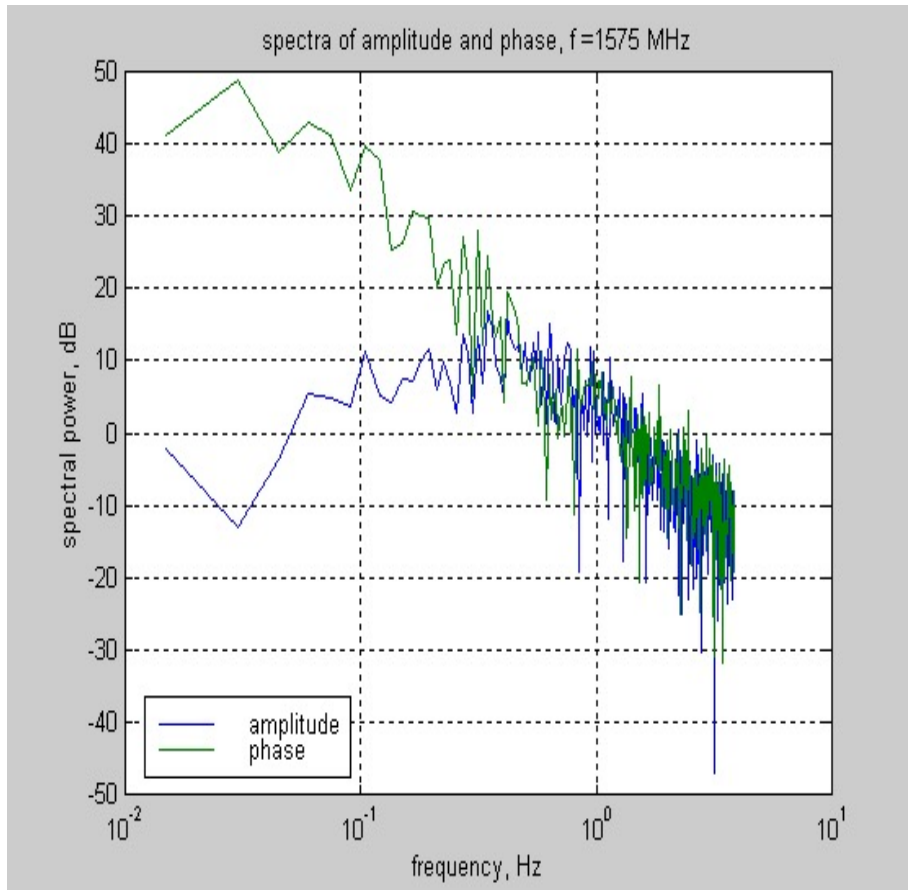
Frequencies $f = 1575$ MHz and 500 MHz.

Time realisations of phase and amplitude on the Earth's surface
 $f = 1575 \text{ MHz}$



Spectra of phase and amplitude fluctuations

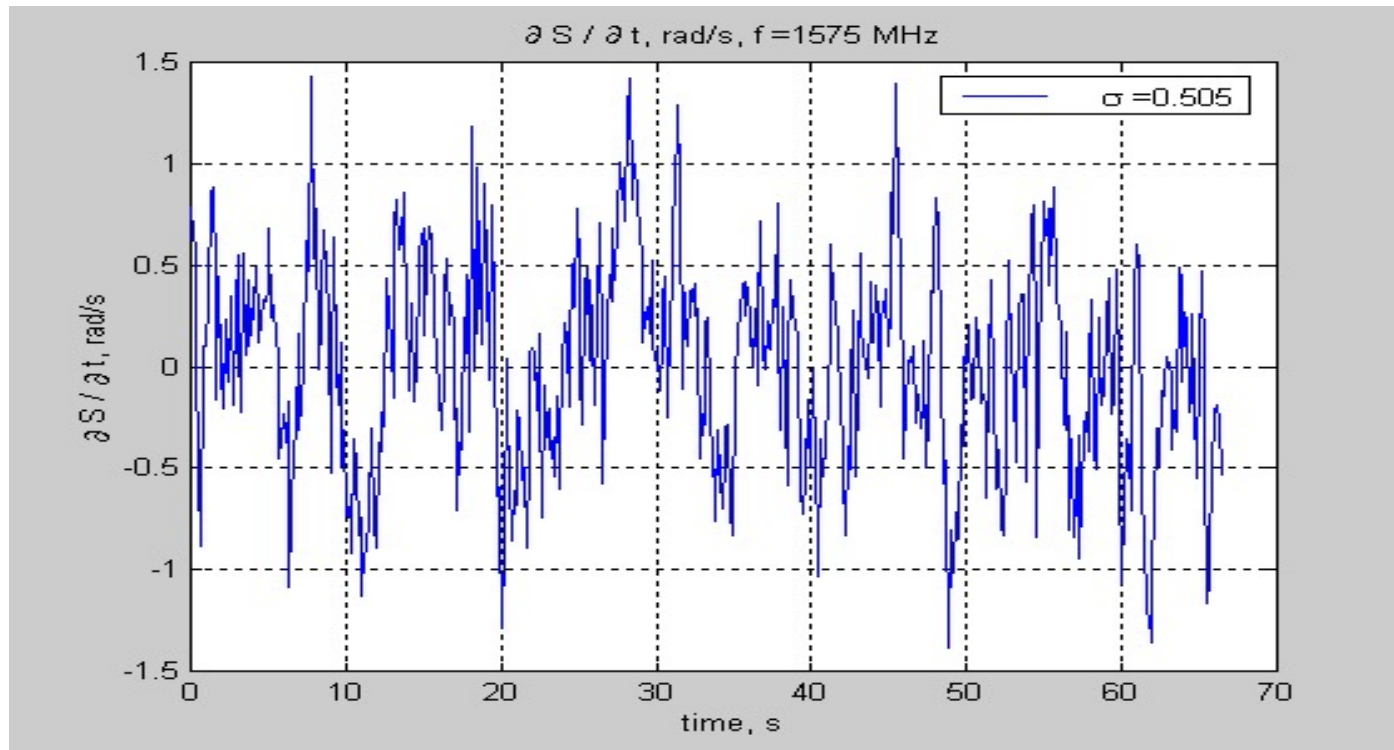
Probability density function of amplitude fluctuations



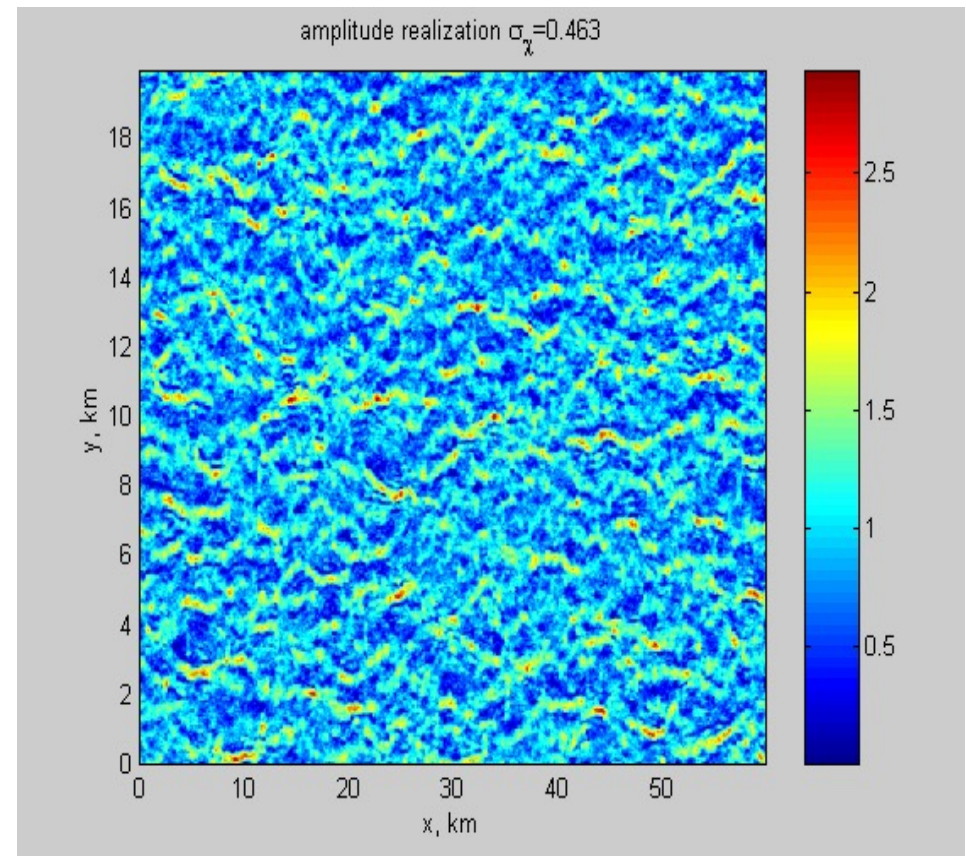
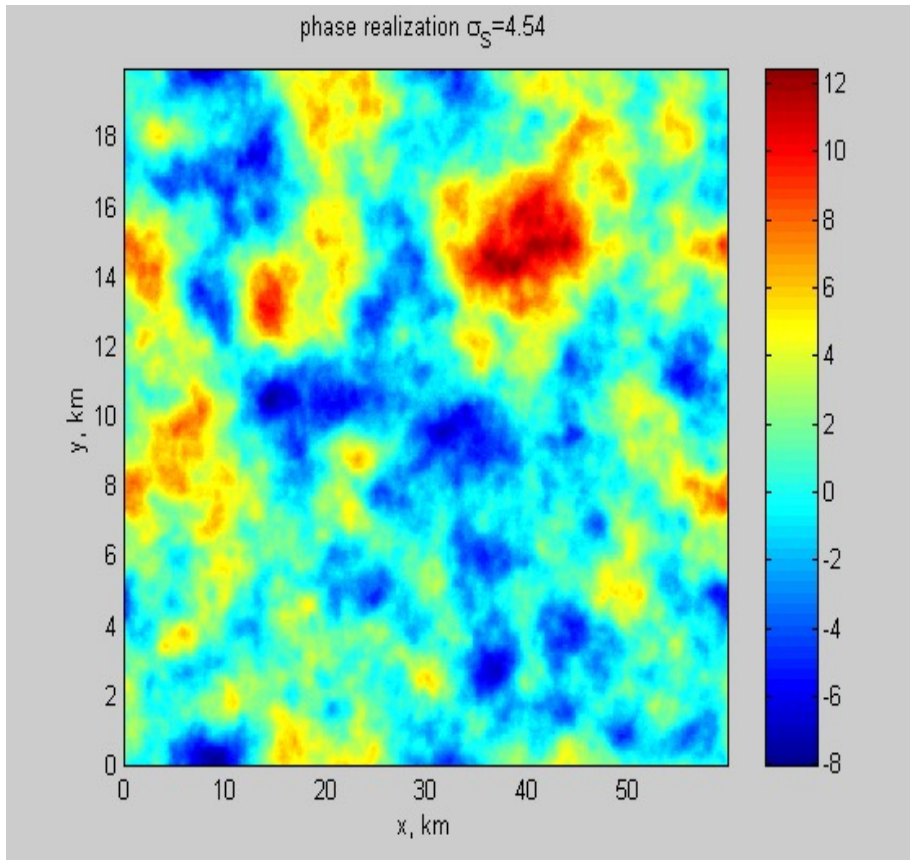
f = 1575 MHz

Rate of phase changes, $f = 1575$ MHz

$$\sigma^2 = \left\langle \left(\frac{\partial S}{\partial t} \right)^2 \right\rangle$$

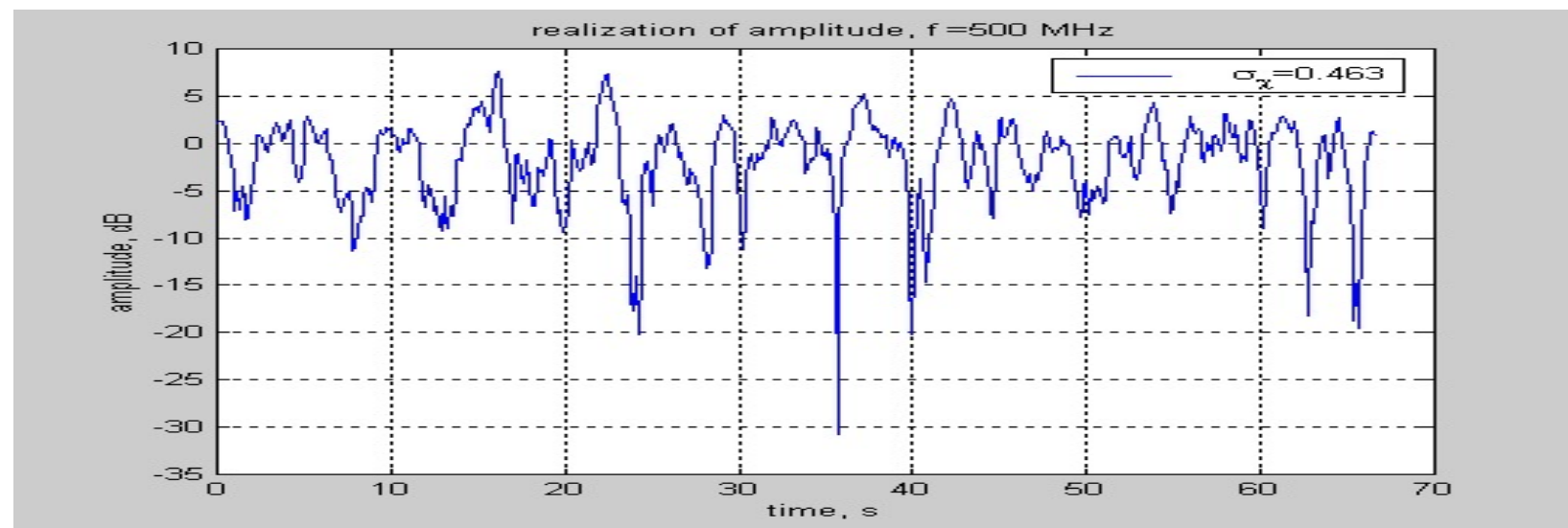
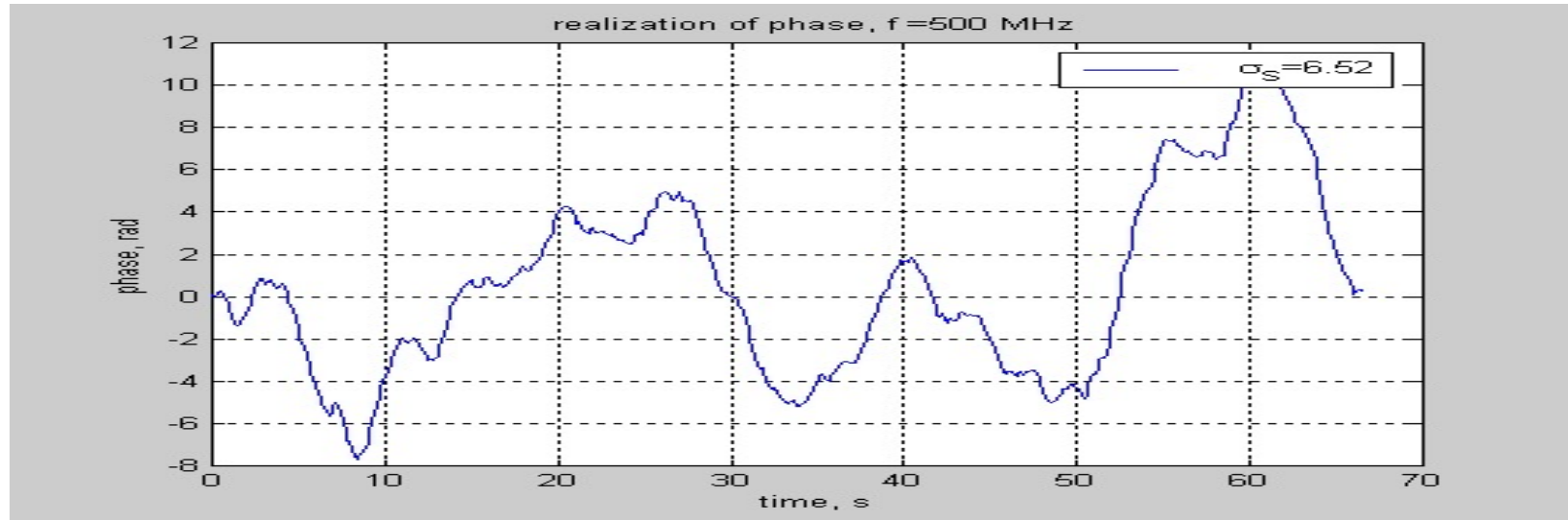


Realisations of phase and amplitude on the Earth's surface.

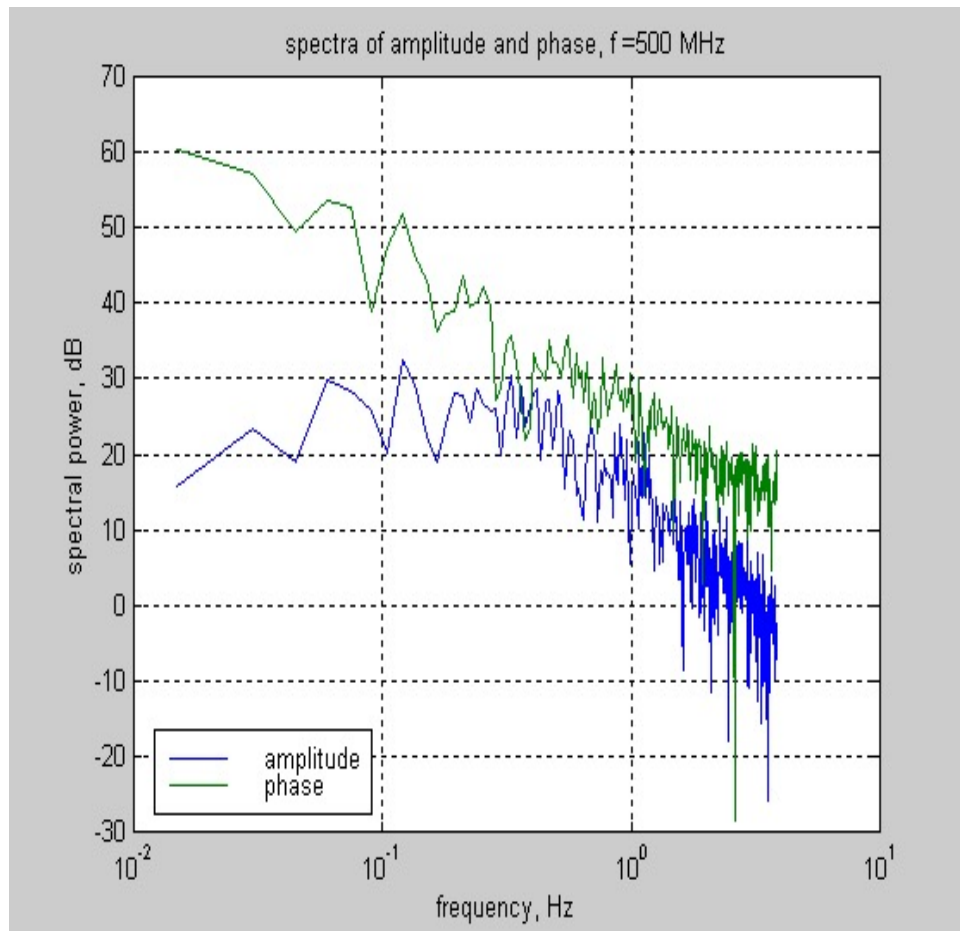


f=500 MHz

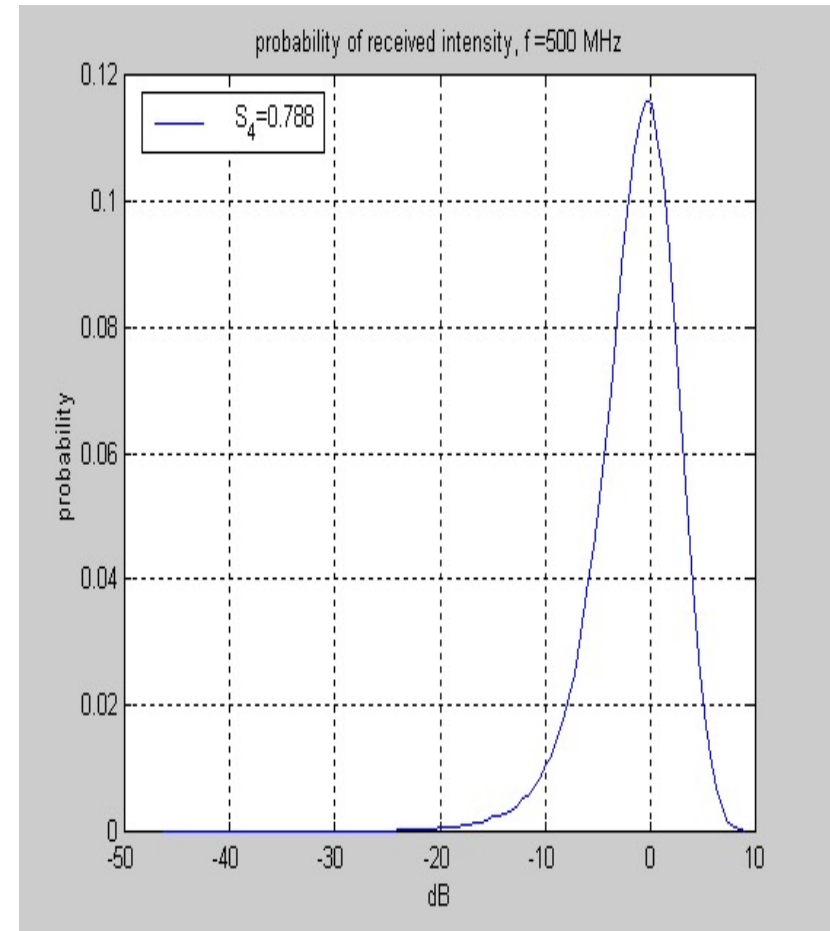
Time realisations of phase and amplitude on the Earth's surface f=500 MHz



Spectra of phase and amplitude fluctuations

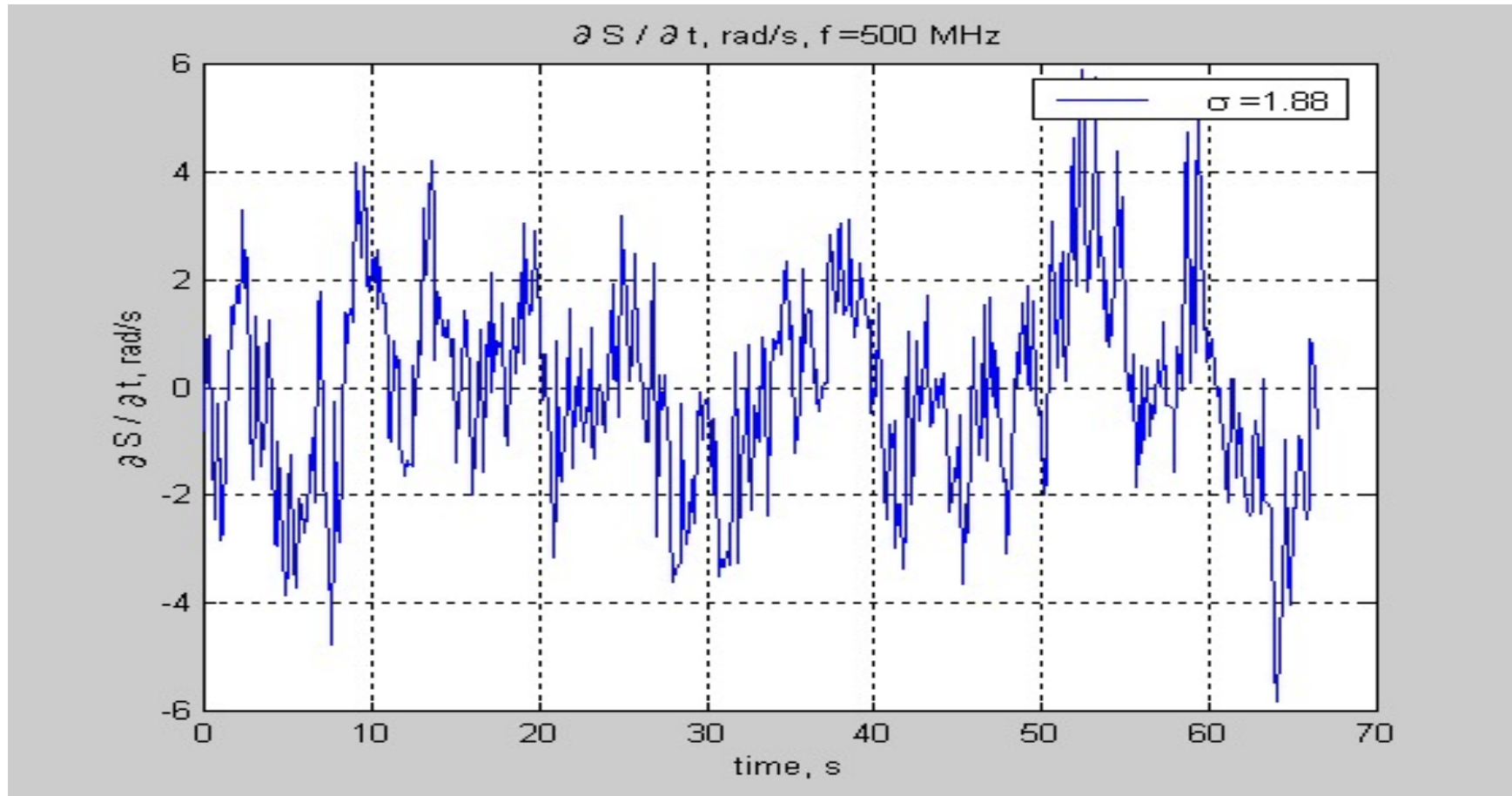


Probability density function of intensity fluctuations



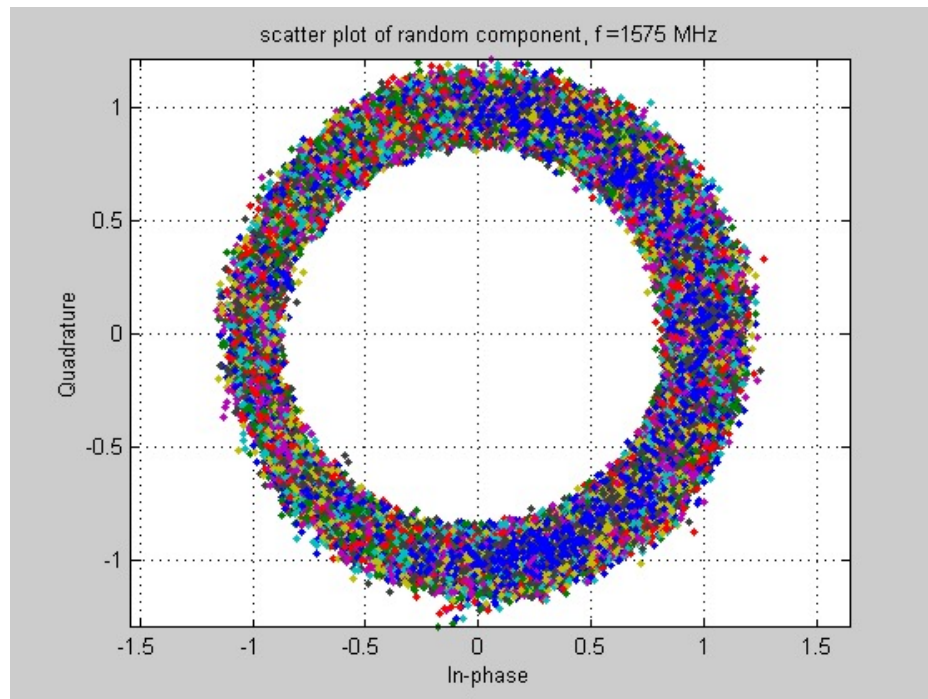
f=500 MHz

Rate of phase changes, $f = 500$ MHz

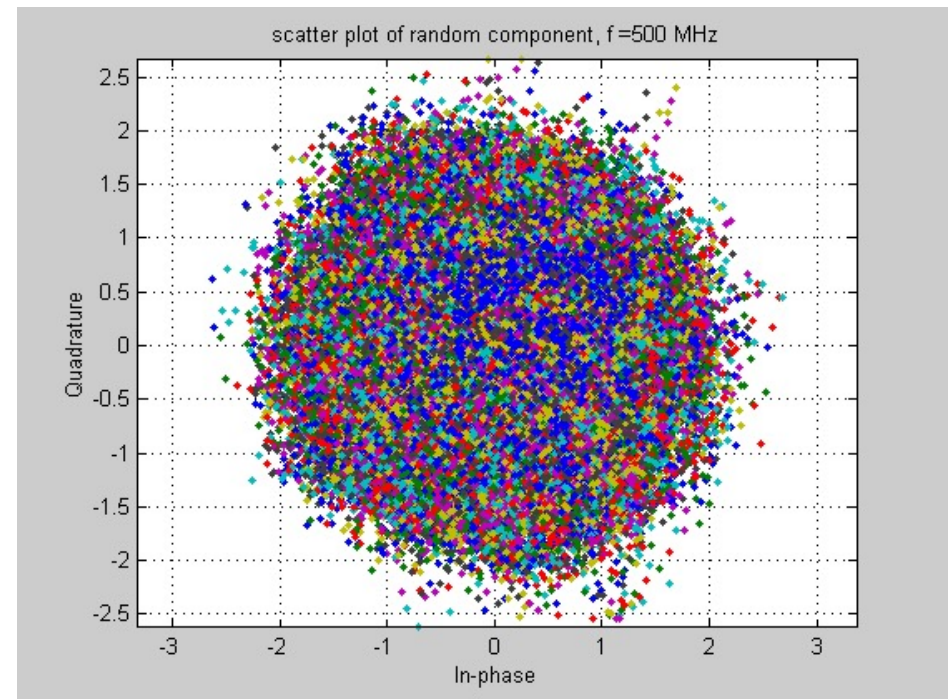


Scatter plots of the complex random factor R

$f=1575$ MHz, $S_4=0.158$



$f=500$ MHz, $S_4=0.768$



To conclude, the presented technique is capable of producing statistical characteristics and of simulating time realisations of the field (including regime of strong amplitude fluctuations) for a wide range of the input parameters, viz:

co-ordinates of the satellite and point of observation

slant electron density profile along a given path

zenith angle of a satellite

magnetic azimuth of the plane of propagation

magnetic field dip angle at the pierce point

the following parameters of the random irregularities:

- spectral index
- outer scale across the geomagnetic field
- aspect ratio
- variance of the fractional electron density fluctuations
- effective velocity of the drift

The field strong scintillation on transionospheric paths of propagation.

Propagation model 2. [2015a,b (8,9)]. Describes the case of strong scintillation already formed in the inhomogeneous ionospheric layer. This technique is based on solving Markov's parabolic equations for the moments of the complex amplitude of the field $U(\mathbf{r}, t) = X(\mathbf{r}, t) + iY(\mathbf{r}, t)$ and does not have formal restrictions imposed on the strength of the field fluctuations. But the distribution of the field remains undefined.

Correlation properties of the field realizations are defined by the moments of the second order – coherence functions

$$\Gamma = \langle U(\mathbf{r}_1, t_1)U^*(\mathbf{r}_2, t_2) \rangle$$

$$\tilde{\Gamma} = \langle U(\mathbf{r}_1, t_1)U(\mathbf{r}_2, t_2) \rangle$$

Auto- and cross-correlation functions of the in-phase and quadrature components

$$\Psi_X = \frac{1}{2} \text{Re}(\Gamma + \tilde{\Gamma}) - \langle U \rangle \langle U \rangle^*,$$

$$\Psi_Y = \frac{1}{2} \text{Re}(\Gamma - \tilde{\Gamma}),$$

$$\Psi_{XY} = \frac{1}{2} \text{Im}(\tilde{\Gamma} - \Gamma).$$

For generating the random realizations of the field some empirical distributions should be employed (e.g. Nakagami, $\alpha - \mu$ distribution), which are somehow governed by S_4 .

Therefore we need to deal with the equations for the moments up to the fourth order.

Markov's parabolic equations for the field moments

- For the mean field

$$\frac{\partial \langle U \rangle}{\partial z} + \frac{k^2}{8} A_\varepsilon(0, z) \langle U \rangle = 0 \quad \rightarrow \quad \langle U(z) \rangle = \exp \left[-\frac{k^2}{8} \int A_\varepsilon(0, z) dz \right],$$

$$A_\varepsilon(x, \tau) = \gamma \Omega_{pl}^4(\tau) \frac{\sqrt{2\pi}}{k_0 2^{\frac{p-5}{2}} \Gamma(\frac{p-3}{2})} \cdot (2\pi x)^{\frac{p-2}{2}} \cdot K_{\frac{p-2}{2}}(2\pi x)$$

- For the second-order coherence function of the first type:

$$\frac{\partial \Gamma}{\partial z} + \frac{k^2}{8} D_\varepsilon(\mathbf{r}, z) \Gamma = 0 \quad \rightarrow \quad \Gamma = \exp \left[-\frac{k^2}{8} \int D_\varepsilon(\mathbf{r}, z) dz \right]$$

- For the second-order coherence function of the second type:

$$\frac{\partial \tilde{\Gamma}}{\partial z} - \frac{i}{k} \nabla^2 \tilde{\Gamma} + \frac{k^2}{4} (A_\varepsilon(0, z) + A_\varepsilon(\mathbf{r}, z)) \tilde{\Gamma} = 0$$

$A_\varepsilon(\mathbf{r}, z)$ - transversal correlation function of permittivity,

$D_\varepsilon(\mathbf{r}, z)$ - transversal structure function of permittivity,

\mathbf{r} – transversal difference variable,

z – co-ordinate in the direction of propagation,

p – spectral index of fluctuations.

In the regime of the moderate and strong scintillation the mean field $\langle U \rangle$ is real-valued and small, and $\tilde{\Gamma}$ is of the order of magnitude of $\langle U \rangle^2$.

Therefore, to the accuracy of the order of $\langle U \rangle \ll 1$ $\Psi_X \approx \Psi_Y \approx \frac{1}{2} \Gamma$, $\Psi_{XY} \approx 0$.

Equation for the fourth moment

$$\frac{\partial \Gamma_4}{\partial z} - \frac{i}{k} \nabla_{\rho_1} \cdot \nabla_{\rho_2} \Gamma_4 + \frac{k^2}{8} F(\boldsymbol{\rho}_1, \boldsymbol{\rho}_2, z) \Gamma_4(\boldsymbol{\rho}_1, \boldsymbol{\rho}_2, z) \Gamma_4 = 0$$

$$F(\boldsymbol{\rho}_1, \boldsymbol{\rho}_2; z) = 2D_\varepsilon(\boldsymbol{\rho}_1, z) + 2D_\varepsilon(\boldsymbol{\rho}_2, z) - D_\varepsilon(\boldsymbol{\rho}_1 + \boldsymbol{\rho}_2, z) - D_\varepsilon(\boldsymbol{\rho}_1 - \boldsymbol{\rho}_2, z)$$

$$S_4^2(z) = \Gamma_4(0, 0; z) - 1$$

$$\zeta = z l_\varepsilon^{-1} \sqrt{kl_\varepsilon}, \quad \mathbf{x}_1 = \boldsymbol{\rho}_1 l_\varepsilon^{-1}, \quad \mathbf{x}_2 = \boldsymbol{\rho}_2 l_\varepsilon^{-1}, \quad \tilde{F} = l_\varepsilon^{-1} F, \quad \tilde{D}_\varepsilon = l_\varepsilon^{-1} D_\varepsilon.$$

$$K \frac{\partial \Gamma_4}{\partial \zeta} - i \nabla_{\mathbf{x}_1} \cdot \nabla_{\mathbf{x}_2} \Gamma_4 + \frac{K^2}{8} \tilde{F}(\mathbf{x}_1, \mathbf{x}_2, \zeta) \Gamma_4 = 0.$$

$$\Gamma(\mathbf{x}_1, \mathbf{x}_2; 0) = 1$$

$$K = (kl_\varepsilon)^{3/2} \gg 1$$

$$\Gamma_4(\mathbf{x}_1, \mathbf{x}_2, \zeta) = \int_{R^4} G(\mathbf{x}_1, \boldsymbol{\alpha}_1; \mathbf{x}_2, \boldsymbol{\alpha}_2; \zeta) \mathbf{d}\boldsymbol{\alpha}_1 \mathbf{d}\boldsymbol{\alpha}_2$$

For Green's function $G(\mathbf{x}_1, \boldsymbol{\alpha}_1; \mathbf{x}_2, \boldsymbol{\alpha}_2; \zeta)$ quasi-classical approximation in terms of the large parameter K is employed.

The main term of the asymptotic

$$G(\mathbf{x}_1, \boldsymbol{\alpha}_1; \mathbf{x}_2, \boldsymbol{\alpha}_2; \zeta) = A_0(\mathbf{x}_1, \boldsymbol{\alpha}_1; \mathbf{x}_2, \boldsymbol{\alpha}_2; \zeta) \exp\left[K\psi(\mathbf{x}_1, \boldsymbol{\alpha}_1; \mathbf{x}_2, \boldsymbol{\alpha}_2; \zeta)\right]$$

Quasi-classic equations for the fourth moment

$$\frac{\partial \psi}{\partial \zeta} - i \nabla_{x_1} \psi \nabla_{x_2} \psi + \frac{1}{8} \tilde{F}(\mathbf{x}_1, \mathbf{x}_2, \zeta) = 0$$

“Eikonal” equation

$$\frac{\partial A_0}{\partial \zeta} - i \nabla_{x_1} A_0 \nabla_{x_2} \psi - i \nabla_{x_2} A_0 \nabla_{x_1} \psi - i A_0 (\nabla_{x_1} \nabla_{x_2}) \psi = 0$$

“Transport” equation

$$\tilde{F}(\mathbf{x}_1(\tau), \mathbf{x}_2(\tau); \tau) = \gamma \Omega_{pl}^4(\tau) f(\mathbf{x}_1(\mathbf{a}_1, \tau), \mathbf{x}_2(\mathbf{a}_2, \tau)). \quad \gamma = \sigma_{fr}^2 \frac{\omega_{pl \max}^4}{\omega^4}; \quad \Omega_{pl}^4(\tau) = \frac{\omega_{pl}^4(\tau)}{\omega_{pl \max}^4}$$

$$\Gamma_4(0, 0, \zeta) = \frac{1}{(2\pi\zeta)^2} \int_{R^4} d\mathbf{a}_1 d\mathbf{a}_2 \cdot$$

$$\exp \left\{ -\frac{i\gamma}{8} \int_0^\zeta \frac{d\tau}{\tau^2} \int_0^\tau d\tau' (\tau')^2 \Omega_{pl}^4(\tau') \frac{\partial^2}{\partial \mathbf{x}_1 \partial \mathbf{x}_2} f \left(\mathbf{a}_1 \left(1 - \frac{\tau'}{\zeta} \right), \mathbf{a}_2 \left(1 - \frac{\tau'}{\zeta} \right) \right) \right\}.$$

$$\exp \left\{ K \left[\frac{i}{\zeta} (\mathbf{a}_1 \cdot \mathbf{a}_2) - \frac{\gamma}{8} \int_0^\zeta \Omega_{pl}^4(\tau) f \left(\mathbf{a}_1 \left(1 - \frac{\tau}{\zeta} \right), \mathbf{a}_2 \left(1 - \frac{\tau}{\zeta} \right) \right) d\tau \right] \right\}$$

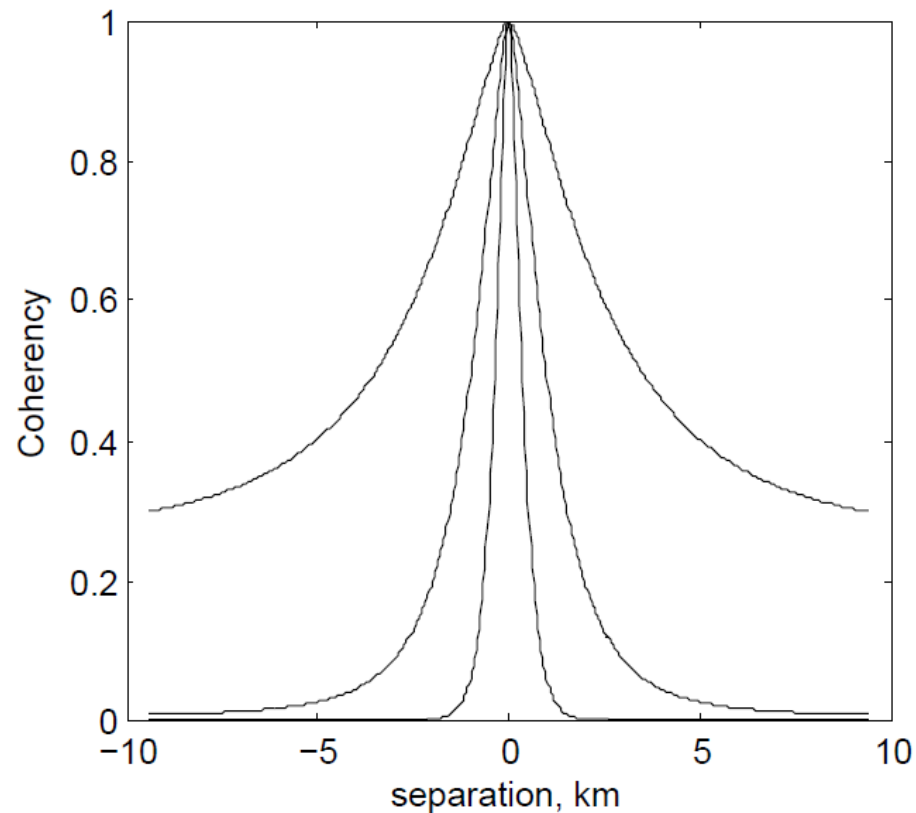
$$S_4^2(\zeta) = \Gamma_4(0, 0; \zeta) - 1$$

Numerical results for the non-homogeneous ionospheric layer, Chapman profile.

Layer height – 350 km, $h_m = 100$ km, $f_{p\ max} = 12$ MHz

Zenith angle 30 deg, slant TEC 124 TECU

Transmission frequency 1200 MHz

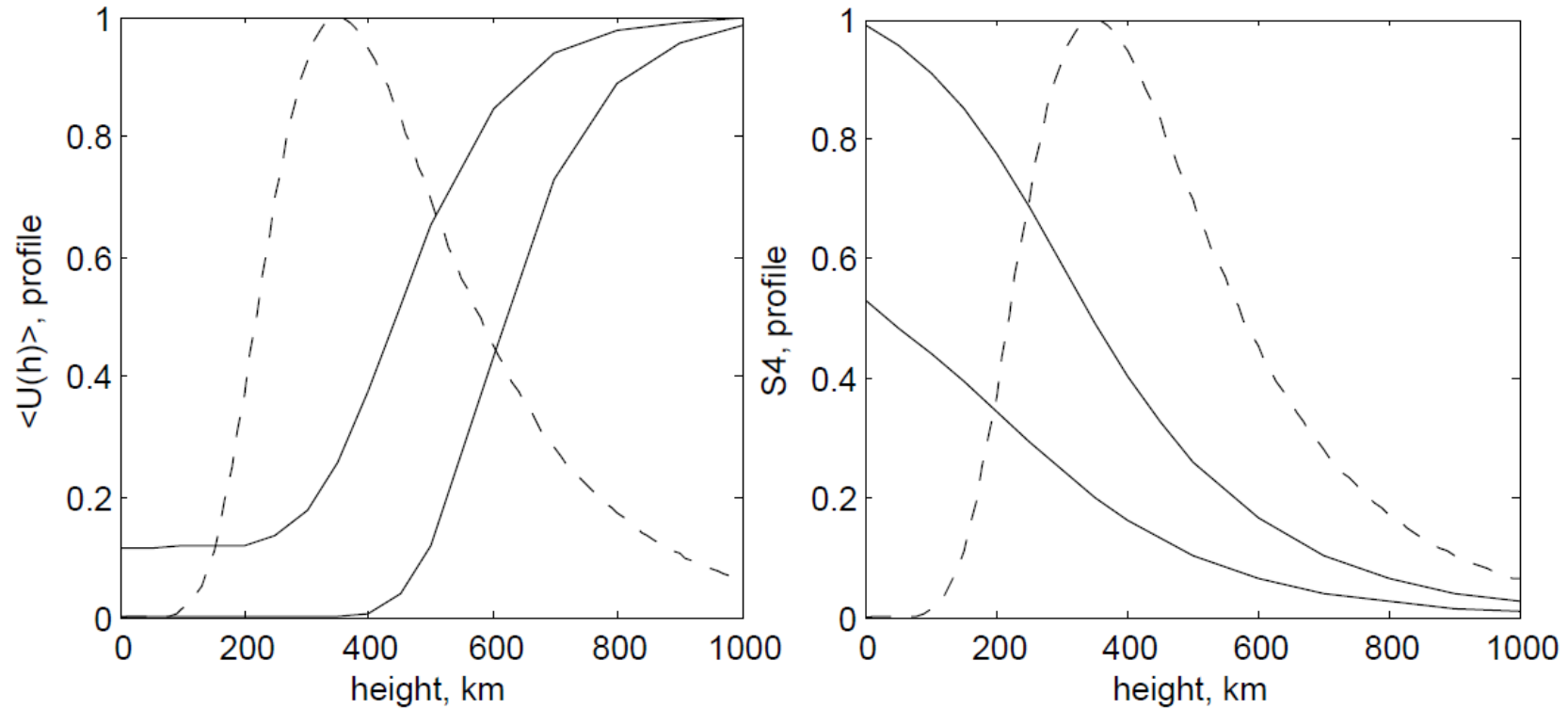


The coherence function Γ
for the point of observation
on the Earth's surface.

Standard deviations of the
fractional electron density
5 %, 10 % and 20 %

The mean field (left) and scintillation index (right) as function of the height above the Earth's surface.

Standard deviations of the fractional electron density – 9 % and 20 %



The physically based software simulator of the scintillating signal

The task for the computer simulator is to generate the random time series having the **given amplitude PDF**, which additionally has the in-phase and quadrature components with the **correlation functions** calculated according to the developed above propagation theory [2015a,b (8,9)].

The procedure of generating the signal is **universal** respectively the type of the amplitude distribution. In the following examples the α - μ distribution [Yacoub, M. (2007), *The α - μ Distribution: A Physical Fading Model for the Stacy Distribution, IEEE Transactions on Vehicular Technology*, 56, 27-34.] is employed which for normalized amplitude b is given by

$$p_m(b) = \frac{\alpha b^{\alpha\mu-1}}{\xi^{\alpha\mu/2} \Gamma(\mu)} e^{-\frac{b^\alpha}{\xi^{\alpha/2}}}, \quad \xi = \frac{\Gamma(\mu)}{\Gamma(\mu + 2/\alpha)}$$

$$\alpha = \alpha(S_4)$$
$$\mu = \mu(S_4)$$

Empirically parameterized by Moraes AO, de Paula ER, Perrella WJ, Rodrigues FS (2012), On the distribution of GPS signal amplitudes during the low-latitude ionospheric scintillation. GPS Solutions doi: 10.1007/s10291-012-0295-3

The general procedure of generating time series of the complex stochastic amplitude U is as follows:

- Two independent random Gaussian processes $\xi(t)$ and $\eta(t)$ with given identical auto-correlation functions Ψ_V are generated. Then the amplitude $a = |V|$ of the complex random process $V(t) = \xi(t) + i\eta(t)$ is governed by the Rice distribution

$$p_n(a) = 2a(1 + K_0)I_0(2a\sqrt{(K_0 + K_0^2)})e^{-K_0 - a^2(1+K_0)}, \quad K_0 = \frac{A^2}{2\sigma^2}$$

- A mapping function $V \rightarrow U$ is constructed which is then applied to the process $V(t)$ producing the new complex random process $U(t)$ having a given distribution of amplitude $p_m(b)$ with $b = |U|$ being the amplitude of the output complex random process $U(t)$.
- Another mapping function $\Psi_U \rightarrow \Psi_V$ is introduced in order to specify the auto-correlation function of the initial process Ψ_V to produce the given auto-correlation of the output process Ψ_U after the transformation $V \rightarrow U$.

The procedure developed provides the specified amplitude distribution and correlation properties of the output process $U(t)$.

Input parameters

Input parameters for the simulator are obtained from the solution to the equations for the moments of the field.

They are:

- Auto-correlation functions of the in-phase and quadrature components

$$\Psi_X \approx \Psi_Y \approx \frac{1}{2} \Gamma$$

- Value of the mean field

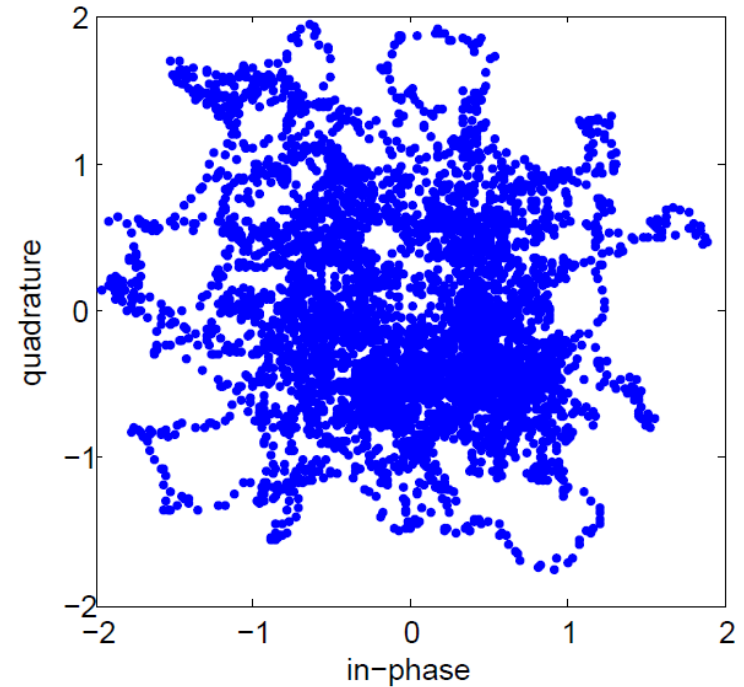
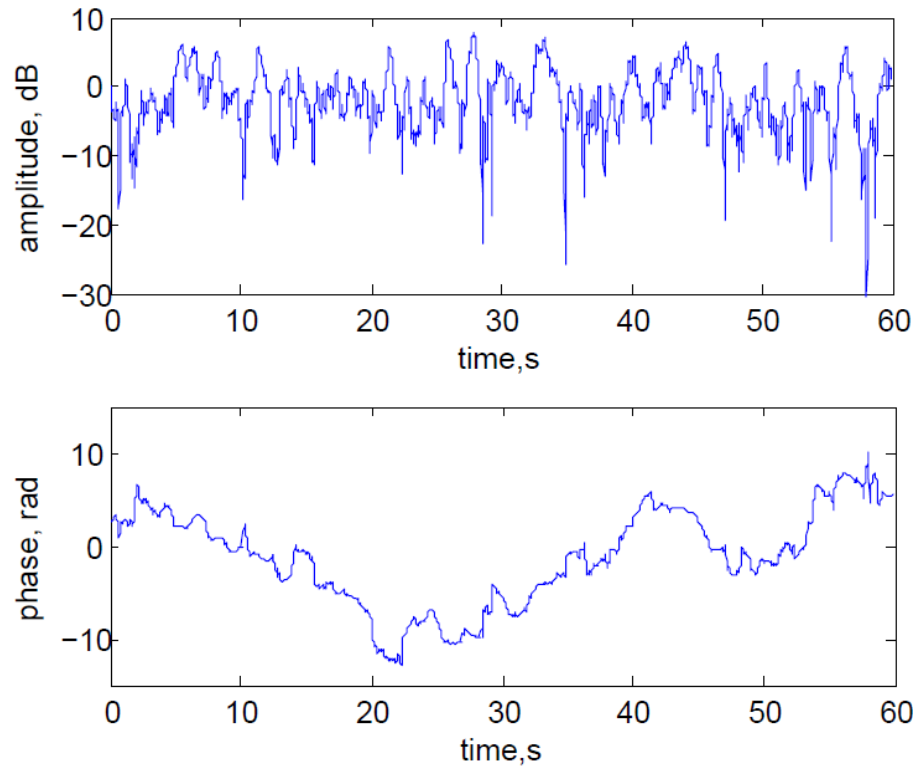
$$\langle U \rangle$$

- Scintillation index

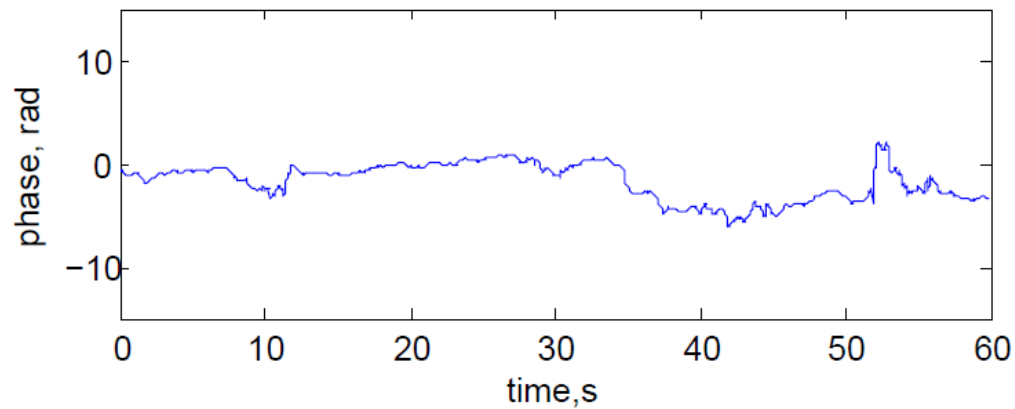
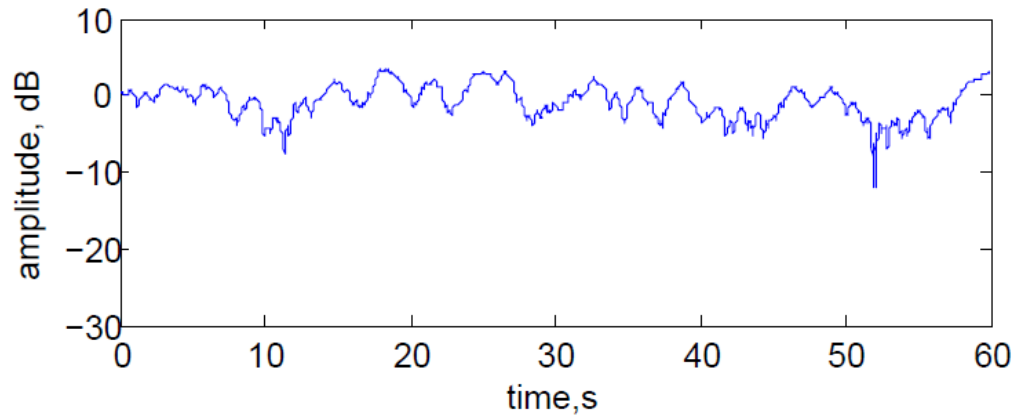
$$S_4 = (\Gamma_4 - 1)^{1/2}$$

Examples of the simulator output

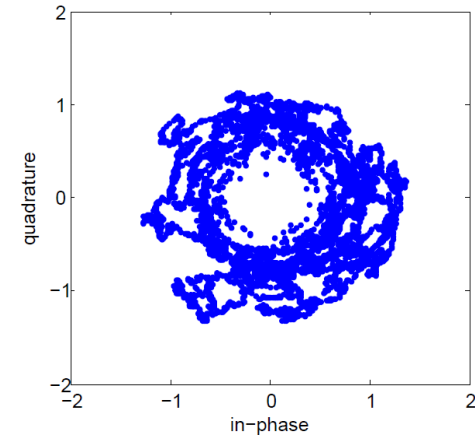
Random time series for the amplitude and phase of the random field on the Earth's surface, generated employing the developed technique; the scintillation index $S_4 = 0.95$, $\langle U \rangle = 0$ (zero-valued random field).



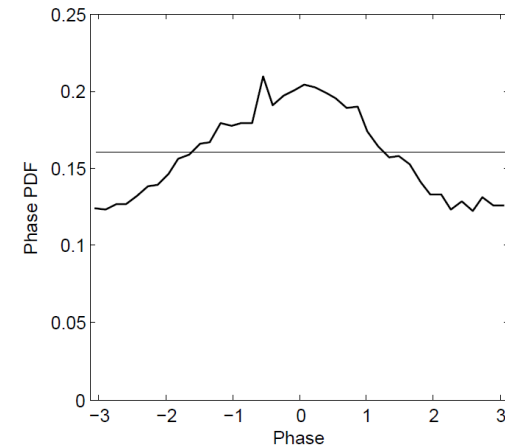
Random walk of the phasor



Random time series for the amplitude and phase of the random field on the Earth's surface, generated employing the developed technique; the scintillation **index $S_4 = 0.53$** , **$\langle U \rangle = 0.12$** (small, but finite value of the mean field).



Random walk of the phasor

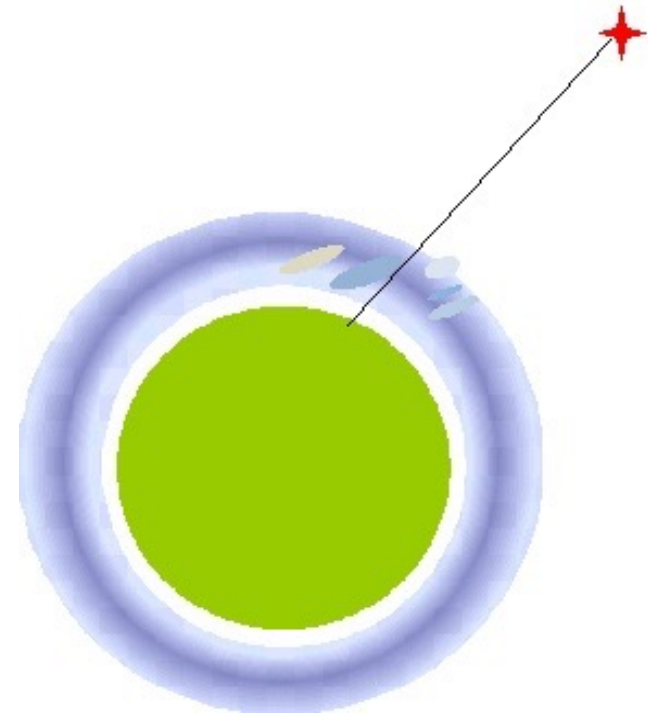


The PDF for the phase distribution.

Strong Scintillation 3. Pulse propagation of VHF field through inhomogeneous stochastic ionosphere

Introduction

- The main goal of this investigation is to present a realistic predominantly analytic theory for solving the problems of the VHF and UHF **pulsed signal propagation** through a realistic transionospheric channel of propagation for different regimes of propagation, including the case of the field strong scintillation.
- «**realistic**» means that for an arbitrary given transionospheric path of propagation the effects of the inhomogeneous background ionosphere are taken into account, including the effect of the Earth's magnetic field.
- The anisotropy in the problem of propagation is taken into account through the anisotropic shapes of local random inhomogeneities of the electron density of the ionosphere.



The geometry of propagation.
The background ionosphere is not necessarily spherically-symmetric

The pulse mean energy

In our consideration the pulse field is characterized by its mean energy, given as follows:

$$W(\mathbf{0}, z, t) = \langle E(\mathbf{0}, z, t) E^*(\mathbf{0}, z, t) \rangle$$

$$= \iint_{-\infty}^{+\infty} d\omega_1 d\omega_2 \Gamma(\mathbf{0}, z, \omega_1, \omega_2) P(\omega_1) P^*(\omega_2) .$$

$$\exp \left\{ i \left[(\omega_1 - \omega_2) \frac{z}{c} - i(\omega_1 - \omega_2)t - \frac{e^2}{2mc\epsilon_0} \left(\frac{1}{\omega_1} - \frac{1}{\omega_2} \right) \int_0^z N_0(\mathbf{0}, z') dz' \right] \right\} . \quad (1)$$

Here $\Gamma(\boldsymbol{\rho} = \mathbf{0}, z, \omega_1, \omega_2)$ is the first second order transversal two-position two-frequency coherence function of the field monochromatic components, propagating through the stochastic ionosphere; $P(\omega)$ is a given spectrum of a launched pulse signal, $N_0(\mathbf{0}, z)$ is the electron density distribution along an arbitrary given path of a pulse propagation, $\boldsymbol{\rho}^2 = \left(\frac{x^2}{a^2(\varphi)} + \frac{y^2}{b^2} \right)$, (x, y, z) are the Cartesian variables, where (x, y) are the transversal difference variables, and z is the variable along the line of sight.

Constructing the analytic solution to the coherence function $\Gamma(\mathbf{0}, z, \omega_1, \omega_2)$

This function is the core point to quantitatively describe the pulse mean energy [2020a,b (11, 12)]. To do it for the field propagation in the regime of strong scintillation, below the appropriate diffusive Markov approximation is used as follows:

$$\frac{\partial \Gamma}{\partial z} + \frac{ik_d}{2(k_s^2 - \frac{1}{4}k_d^2)} \nabla_{\perp}^2 \Gamma + \frac{(k_s^2 - \frac{1}{4}k_d^2)}{8} D_{\varepsilon}(\boldsymbol{\rho}, z, \varphi, \omega_1, \omega_2) \Gamma = 0 \quad (2)$$

$$k_d = \frac{\omega_1 - \omega_2}{c}, \quad k_s = \frac{\omega_1 + \omega_2}{2c}.$$

$D_{\varepsilon}(\boldsymbol{\rho}, z, \varphi, \omega_1, \omega_2)$ is the transversal two position and two-frequency structure function of the dielectric permittivity fluctuations

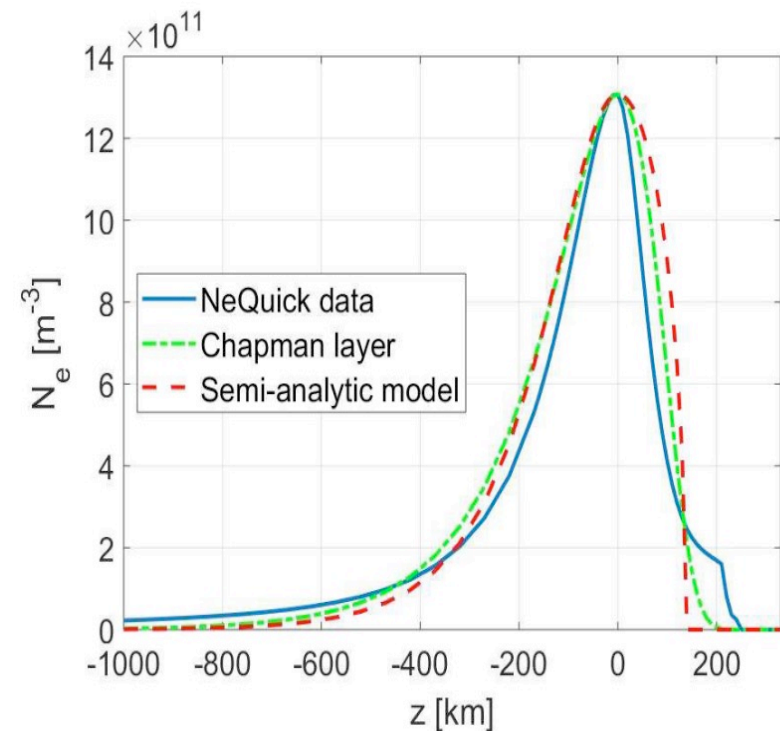
To further solve the equation (2), first, the semi-analytic model of the background ionosphere is introduced as shown in Figure below

The distribution of the electron density along the line of sight in the background ionosphere is specified by one of the known standard ionospheric models (NeQuick, blue curve).

A semi-analytic model of this distribution is then introduced, which permits further constructing the rigorous analytic solution to equation (2) (red dashed curve). It provides the same values of TEC and N_e in the maximum of the layer as in the model, generated by NeQuick.

Here the top side ionospheric half-layer is modeled by half-parabola, and the bottom side is presented by hyperbolic cosine (see details in 2020a,b).

The semi-analytic model permits further constructing the rigorous analytic solution to equation (2) with the introduced here parabolic structure function.



The model of the structure function

For the following consideration, the structure function of fluctuations of the dielectric permittivity $D_\varepsilon(\boldsymbol{\rho}, z, \varphi, \omega_1, \omega_2)$ of the ionosphere is accepted in the form of the Gaussian beam as follows the parabolic function in the directions orthogonal the line of sight

$$D_\varepsilon(\boldsymbol{\rho}, z, \varphi, \omega_1, \omega_2) = \frac{2k_{pl}^4(z)\sigma_N^2 l_\varepsilon(\varphi)}{\left(k_s^2 - \frac{1}{4}k_d^2\right)^2} \boldsymbol{\rho}^2(x, y), \quad \boldsymbol{\rho}^2 = \left(\frac{x^2}{a^2(\varphi)} + \frac{y^2}{b^2}\right), \quad (3)$$
$$k_{pl}^2(z) = \frac{e^2 n(z)}{\varepsilon_0 c^2 m_e}$$

Parameter $l_\varepsilon(\varphi)$ is the effective correlation radius of the electron density fluctuations in the direction of propagation.

φ is the angle between the direction of pulse propagation (line of sight) and the Earth magnetic field at the pierce point

Calibration of the parabolic structure function $D_\varepsilon(\boldsymbol{\rho}, z, \varphi, \omega_1, \omega_2)$

- To take account of the realistic inverse power law spectrum of fluctuations of the electron density of the ionosphere, the Gaussian structure function (3) should be properly calibrated in order to further obtain the solution to the problem of the pulse transionospheric propagation, which is in compliance with the inverse power law spectrum of the ionospheric electron density fluctuations. To do this, the solution to the pure spatial coherence function is employed, which was earlier obtained in [2020a,b], independently of the theory, which is developed here. This solution is as follows:

- $$\Gamma(\boldsymbol{\rho}, z, \varphi) = \Gamma(\boldsymbol{\rho}, 0, \varphi) \exp\left[-\frac{k_s^2}{8} \int_0^z D_\varepsilon(\boldsymbol{\rho}, z', \varphi) dz'\right].$$

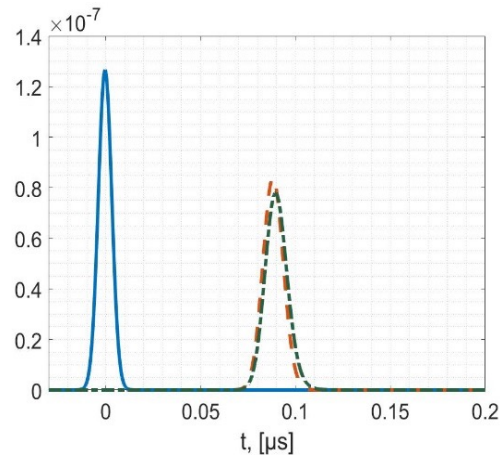
As the result, the two-frequency coherence function (zero space separation) along the path of propagation, properly corresponding to the appropriate inverse power law spectrum of fluctuations of the electron density, which is further employed for calculating the pulse mean energy is as follows [2020a,b (11, 12)]:

$$\Gamma_t(0,0; z; \varphi) = \frac{1}{\sqrt{\psi_{1t}(z) \psi_{2t}(z)}} \exp \left\{ - \frac{\sigma_N^2 l_\varepsilon(\varphi) k_d^2 k_{plm}^4}{8 \left(k_s^2 - \frac{1}{4} k_d^2 \right)^2} l_t \left[1 + \tanh \left(\frac{z}{l_t} \right) \right] \right\} \quad \begin{array}{l} \text{Top-side} \\ \text{ionosphere} \end{array}$$

$$\Gamma_b(0,0; z; \varphi) = \frac{1}{\sqrt{\psi_{1b}(z) \psi_{2b}(z)}} \exp \left\{ - \frac{\sigma_N^2 l_\varepsilon(\varphi) k_d^2 k_{plm}^4}{8 \left(k_s^2 - \frac{1}{4} k_d^2 \right)^2} l_t \left[1 + \frac{z}{l_t} \left(1 - \frac{z^2}{3l_b^2} \right) \right] \right\} \quad \begin{array}{l} \text{Bottom-side} \\ \text{ionosphere} \end{array}$$

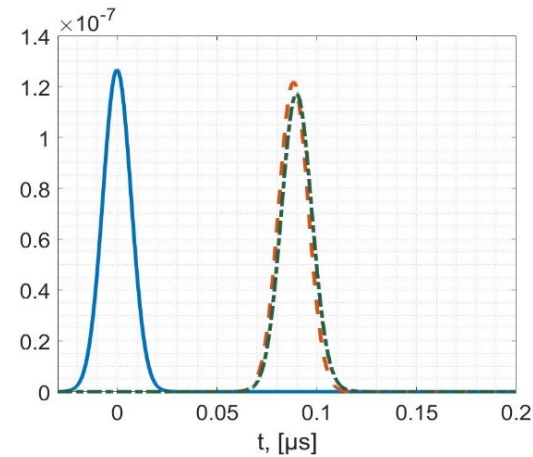
$$\Gamma_v(0,0; z; \varphi) = \frac{1}{\sqrt{\psi_{1b}(l_b) \psi_{2b}(l_b) \chi_1(z) \chi_2(z)}} \exp \left\{ - \frac{\sigma_N^2 l_\varepsilon(\varphi) k_d^2 k_{plm}^4}{8 \left(k_s^2 - \frac{1}{4} k_d^2 \right)^2} l_t \left(1 + \frac{2}{3} \frac{l_b}{l_t} \right) \right\} \quad \begin{array}{l} \text{Atmospheric} \\ \text{layer under the} \\ \text{ionosphere} \end{array}$$

The pulse mean energy. Numerical Results.



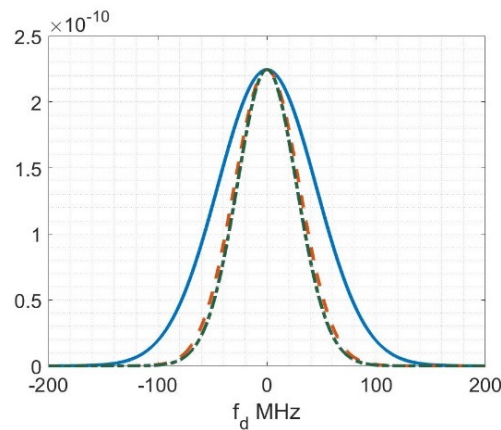
The carrier frequency is 1 GHz.

The length of the input pulse is $5 \cdot 10^{-9}$ s

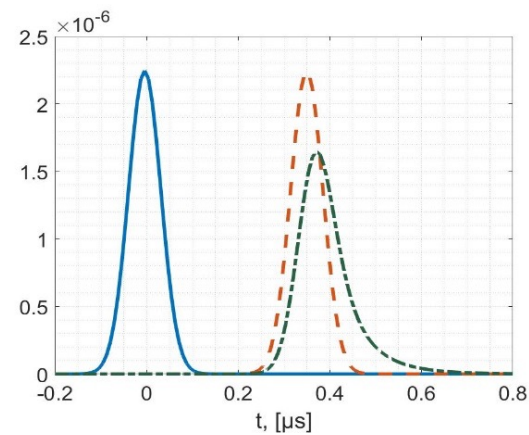


The carrier frequency is 1 GHz.

The length of the input pulse is 10^{-8} s.



The spectrum of the energy of the pulses above



The carrier frequency is 0.5 GHz.

The length of the input pulse is $5 \cdot 10^{-8}$ s.

Conclusions to pulse propagation

- The analytical and numerical theory was presented for describing the VHF and UHF pulse propagation in the stochastic transionospheric channel for the conditions of the field strong scintillation.
- This theory permits modeling pulse propagation for arbitrary given inhomogeneous background ionosphere and anisotropically shaped fluctuations of the ionospheric electron density.
- The core point in the presented theory was building the two-frequency coherence function of the monochromatic components of the pulsed signal. The theory to construct this quantity was developed in the papers [2000 (1), 2005(2)].

Extended Treatment of Statistical Moments of Random Fields in Nonlocal Markov Approximation [2021a,b (13,14); 2022 (15)]

- In the theory of wave propagation in random media, when studying the statistical moments of the propagating field in the conditions of strong scintillation, the approach is widely used, which is based on the diffusive Markov moment equations.
- In this approach the closed form equations for the field moments are derived in the approximation of the delta-correlated fluctuations of the medium.
- To account for the effects of finite values of the longitudinal correlation length of fluctuations of the medium of propagation, the appropriate non-local (integro-differential) equations should be considered.

In particular, such the non-local equation for the mean field can be found in classic books Tatarskij, et. al. [1978], Ishimaru [1978], Klyatskin [1980]. Along with this, we could never find any solution to this equation.

S.M.Rytov, Yu.A.Kravtsov, V.I.Tatarskii. *Introduction to Statistical Radiophysics*
V.I.Klyatskin. *Stochastic Equations and Waves in Randomly-Inhomogeneous Media*
A.Ishimaru. *Wave Propagation and Scattering in Random Media*

The equations for the mean field

$$\frac{\partial \langle v \rangle}{\partial z} - \frac{i}{2k} \Delta_{\perp} \langle v \rangle + \frac{k^2}{8} A_{\varepsilon}(z, \boldsymbol{\rho}, \boldsymbol{\rho}) \langle v \rangle = 0$$

Markov parabolic equation

This is the approximation of the delta-correlated random field in the direction of propagation.

$$\psi_{\varepsilon}(z, \boldsymbol{\rho}, z', \boldsymbol{\rho}') \rightarrow \psi_{\varepsilon}^{eff}(z, \boldsymbol{\rho}, z', \boldsymbol{\rho}') = \delta(z - z') A_{\varepsilon}(z, \boldsymbol{\rho}, \boldsymbol{\rho}')$$

$$A_{\varepsilon}(z, \boldsymbol{\rho}, \boldsymbol{\rho}') = \int_{-\infty}^{\infty} \psi_{\varepsilon}(z, \boldsymbol{\rho}, z', \boldsymbol{\rho}') dz' = \frac{\omega_p^4(z, \boldsymbol{\rho})}{\omega^4} A_N(\boldsymbol{\rho} - \boldsymbol{\rho}')$$

The integro-differential equation

$$\frac{\partial \langle v \rangle}{\partial z} - \frac{i}{2k} \Delta_{\perp} \langle v \rangle + \frac{k^2}{4} \int_0^z dz' \psi_{\varepsilon}(z, \boldsymbol{\rho}, z', \boldsymbol{\rho}) \langle v(z', \boldsymbol{\rho}) \rangle \exp \left\{ -\frac{k^2}{8} \int_{z'}^z A_{\varepsilon}(z'', \boldsymbol{\rho}, \boldsymbol{\rho}) dz'' \right\} = 0$$

$$\psi_{\varepsilon}(z, \boldsymbol{\rho}, z', \boldsymbol{\rho}) = \frac{\omega_p^4(z, \boldsymbol{\rho})}{\omega^4} B_N(z - z', \mathbf{0})$$

$$A_{\varepsilon}(z, \boldsymbol{\rho}, \boldsymbol{\rho}) = \int_{-\infty}^{\infty} \psi_{\varepsilon}(z, \boldsymbol{\rho}, z', \boldsymbol{\rho}) dz' = \frac{\omega_p^4(z, \boldsymbol{\rho})}{\omega^4} A_N(\mathbf{0})$$

The first second-order transverse spaced position coherence function

$$\Gamma(\boldsymbol{\rho}_1, \boldsymbol{\rho}_2, z) = \langle v(\boldsymbol{\rho}_1, z)v^*(\boldsymbol{\rho}_2, z) \rangle$$

Markov parabolic equation for $\Gamma(\boldsymbol{\rho}_1, \boldsymbol{\rho}_2, z)$

$$\frac{\partial \Gamma}{\partial z} + \frac{1}{2ik} (\Delta_{\boldsymbol{\rho}_1} - \Delta_{\boldsymbol{\rho}_2})\Gamma + \frac{k^2}{8} \Phi_h(\boldsymbol{\rho}_1 - \boldsymbol{\rho}_2, z)\Gamma = 0$$

$$\Phi_h(\boldsymbol{\rho}, z) = \int_{-\infty}^{+\infty} \varphi_h(\boldsymbol{\rho}, z - z', z) dz' \quad \text{Effective transversal structure function}$$

$$\varphi_h(\boldsymbol{\rho}, z - z', z) = \frac{\omega_p^4(z, \boldsymbol{\rho})}{\omega^4} (2B_N(0, z - z') - 2B_N(\boldsymbol{\rho}, z - z'))$$

Non-local integro-differential equation

$$\frac{\partial \Gamma}{\partial z} + \frac{1}{2ik} (\Delta_{\boldsymbol{\rho}_1} - \Delta_{\boldsymbol{\rho}_2})\Gamma + \frac{k^2}{4} \int_0^z \varphi_h(\boldsymbol{\rho}_1 - \boldsymbol{\rho}_2, z, z - z')\Gamma(\boldsymbol{\rho}_1, \boldsymbol{\rho}_2, z') \exp \left\{ -\frac{k^2}{8} \int_{z'}^z \Phi_h(\boldsymbol{\rho}_1 - \boldsymbol{\rho}_2, z'') dz'' \right\} dz' = 0$$

Simplified equations for the statistical moments

For the case of the incident field in the form of a **plane wave** propagating in z-direction in the **transversally layered** medium, further simplifications in these equations can be performed.

$$\varepsilon_0 = \varepsilon_0(z) \quad \langle v \rangle = \langle v(z) \rangle$$

$$\frac{\partial \langle v \rangle}{\partial z} + \frac{k^2 \omega_p^4(z)}{8 \omega^4} A_N(\mathbf{0}) \langle v \rangle = 0 \quad \longrightarrow \quad \langle v(z) \rangle = \exp \left\{ -\frac{k^2 A_N(\mathbf{0})}{8} \int_{z'}^z \frac{\omega_p^4(z'')}{\omega^4} dz'' \right\}$$

$$\frac{\partial \langle v \rangle}{\partial z} + \frac{k^2}{4} \int_0^z dz' \frac{\omega_p^4(z)}{\omega^4} B_N(z - z', \mathbf{0}) \langle v(z') \rangle \exp \left\{ -\frac{k^2 A_N(\mathbf{0})}{8} \int_{z'}^z \frac{\omega_p^4(z'')}{\omega^4} dz'' \right\} = 0$$

$$\Gamma = \Gamma(\boldsymbol{\rho}, z) \quad \boldsymbol{\rho} = \boldsymbol{\rho}_1 - \boldsymbol{\rho}_2$$

$$\frac{\partial \Gamma}{\partial z} + \frac{k^2}{8} \Phi_h(\boldsymbol{\rho}, z) \Gamma = 0 \quad \longrightarrow \quad \Gamma(\boldsymbol{\rho}, z) = \exp \left\{ -\frac{k^2}{8} \int_0^z \Phi_h(\boldsymbol{\rho}, z'') dz'' \right\}$$

$$\frac{\partial \Gamma}{\partial z} + \frac{k^2}{4} \int_0^z \varphi_h(\boldsymbol{\rho}, z, z - z') \Gamma(\boldsymbol{\rho}, z') \exp \left\{ -\frac{k^2}{8} \int_{z'}^z \Phi_h(\boldsymbol{\rho}, z'') dz'' \right\} dz' = 0$$

The correlation function of the exponential type

The explicit analytic solution to the integro-differential equations can be obtained for the exponential model of the fluctuations of the form:

$$B_N(z - z', \boldsymbol{\rho}) = \frac{A_N(\boldsymbol{\rho})}{2l_{\parallel}} e^{-\frac{|z-z'|}{l_{\parallel}}}$$

$$\varphi_h(\boldsymbol{\rho}, z - z', z) = \frac{\Phi_h(\boldsymbol{\rho}, z)}{2l_{\parallel}} e^{-\frac{|z-z'|}{l_{\parallel}}}, \quad \Phi_h(\boldsymbol{\rho}, z) = \frac{\omega_p^4(z)}{\omega^4} (2A_N(0) - 2A_N(\boldsymbol{\rho}))$$

Here $\boldsymbol{\rho} = \boldsymbol{\rho}_1 - \boldsymbol{\rho}_2$, l_{\parallel} is the longitudinal correlation radius of the electron density fluctuations. For this model the explicit solutions to the equations are obtained in general case of the medium which is **non-homogeneous** in the direction of propagation.

$$\langle v(z) \rangle = \exp \left[-\frac{k^2 A_N(0)}{8} \int_0^z \frac{\omega_p^4(z')}{\omega^4} dz' \right] + \frac{k^2 A_N(0)}{8} \int_0^z \frac{\omega_p^4(z')}{\omega^4} \exp \left[-\frac{z'}{l_{\parallel}} - \frac{k^2 A_N(0)}{8} \int_{z'}^z \frac{\omega_p^4(z'')}{\omega^4} dz'' \right] dz'$$

$$\Gamma(\boldsymbol{\rho}, z) = \exp \left[-\frac{k^2}{8} \int_0^z \Phi_h(\boldsymbol{\rho}, z') dz' \right] + \frac{k^2}{8} \int_0^z \Phi_h(\boldsymbol{\rho}, z') \exp \left[-\frac{z'}{l_{\parallel}} - \frac{k^2}{8} \int_{z'}^z \Phi_h(\boldsymbol{\rho}, z'') dz'' \right] dz'$$

Explicit representation for the mean field in the case of the exponential model and homogeneous background medium

$$\psi_\varepsilon(0, s, l_{\parallel}) = \frac{A_\varepsilon(0)}{2l_{\parallel}} e^{-\frac{|s|}{l_{\parallel}}}$$

$$2 \int_0^{\infty} \psi_\varepsilon(0, s) ds = A_\varepsilon(0)$$

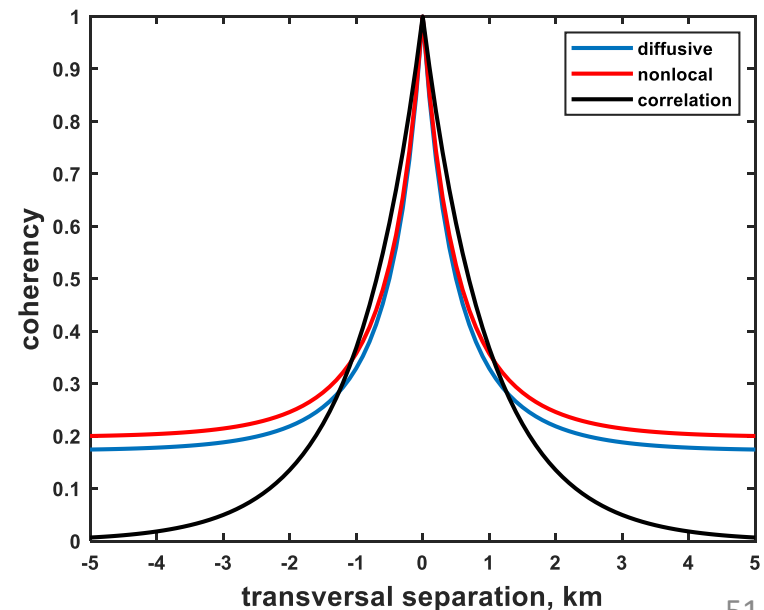
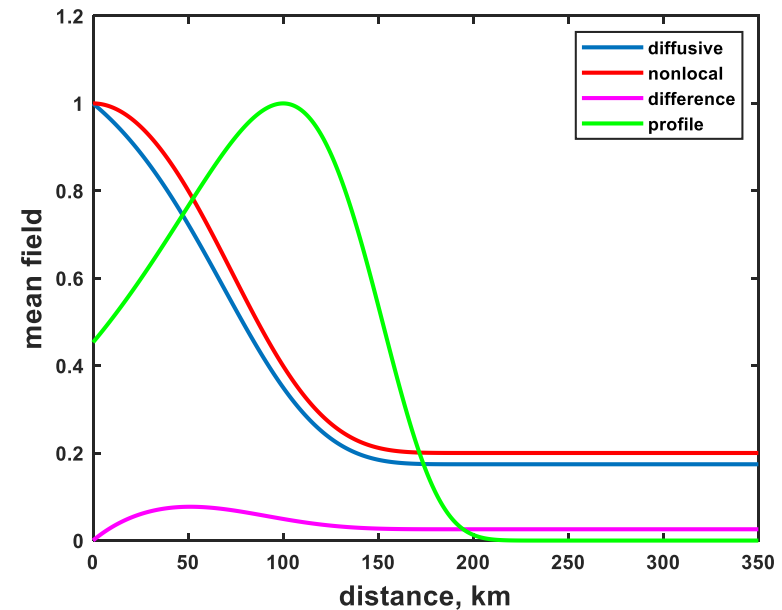
$$\frac{d \langle v \rangle}{ds} + \frac{A_\varepsilon(0)}{8l_{\parallel}} \int_0^s e^{-\frac{s-s'}{l_{\parallel}}} e^{-\frac{1}{8}A_\varepsilon(0)(s-s')} \langle v(s') \rangle ds' = 0$$

$$\langle v \rangle = \frac{1}{1 - \frac{A_\varepsilon(0)l_{\parallel}}{8}} e^{-\frac{A_\varepsilon(0)}{8}s} + \frac{\frac{A_\varepsilon(0)l_{\parallel}}{8}}{\frac{A_\varepsilon(0)l_{\parallel}}{8} - 1} e^{-\frac{s}{l_{\parallel}}}$$

$$\langle v \rangle = e^{-\frac{k^2 A_{\varepsilon, \rho}(0)}{8} z} \quad (\text{the limiting case of } l_{\parallel} = 0)$$

An example. Propagation through the non-homogeneous ionospheric layer

- The plasma layer was specified by the Chapman profile with critical frequency 10 MHz and scale height 40 km.
- The transmission frequency was 1000 MHz.
- The fluctuations of the fractional electron density were supposed to be a spatially homogeneous stochastic field with standard deviation of 0.02 and correlation function specified by the anisotropic exponential model with different vertical and horizontal scales (20 km and 1 km, respectively)



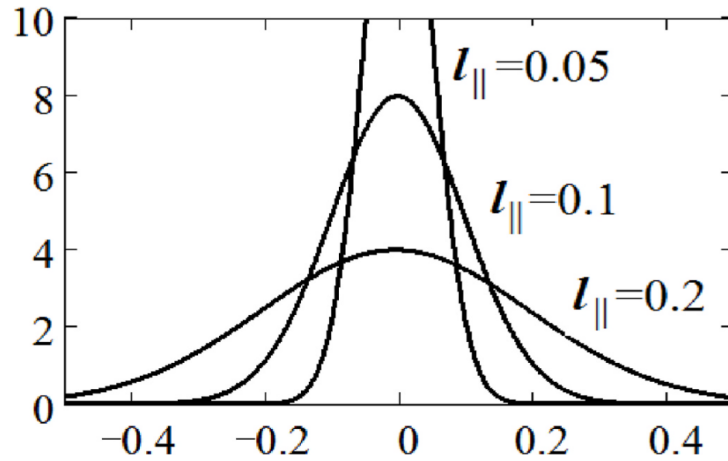


Fig. 1. Correlation function at various values of correlation radius l

$$\psi_{\varepsilon}(0, s; l_{\parallel}) = \sqrt{\frac{1}{2\pi} \frac{A_{\varepsilon}(0)}{l_{\parallel}}} e^{-\frac{s^2}{2l_{\parallel}^2}}.$$

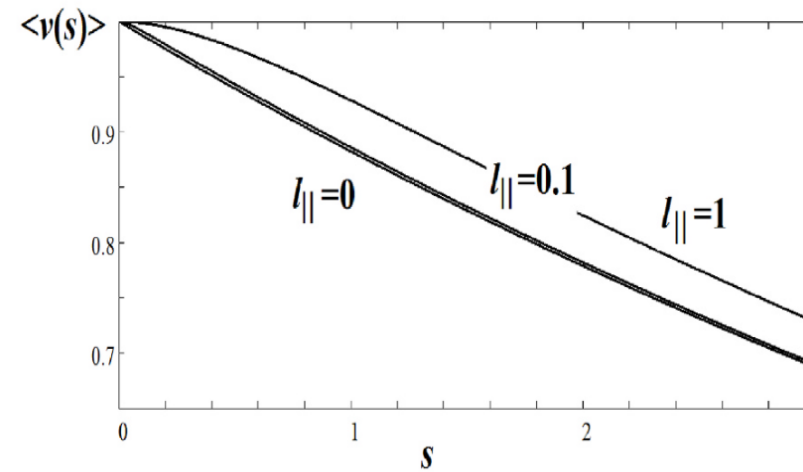
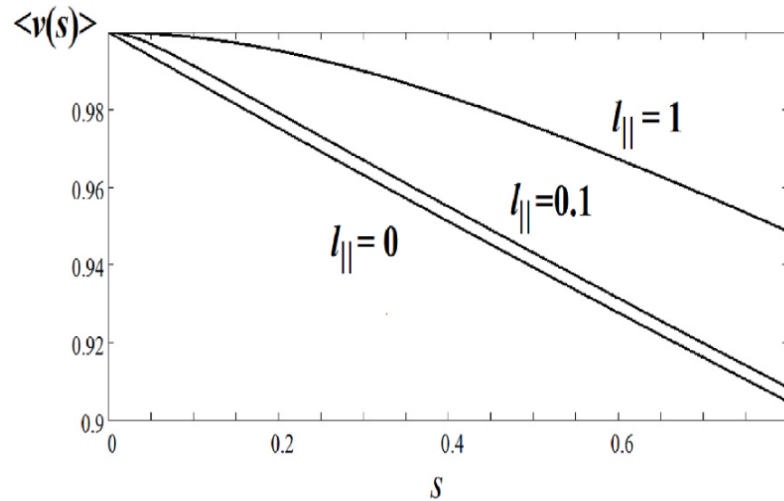
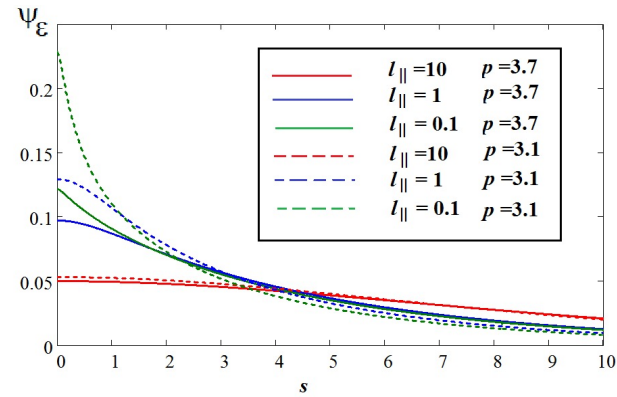
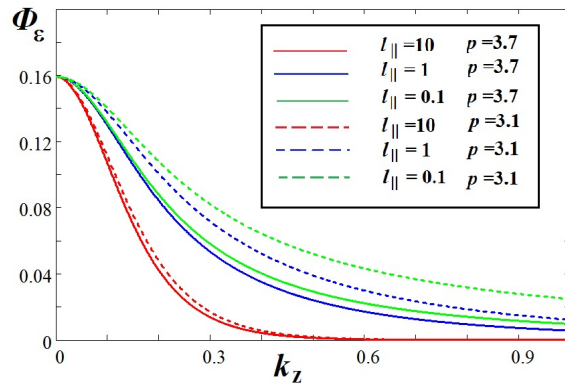
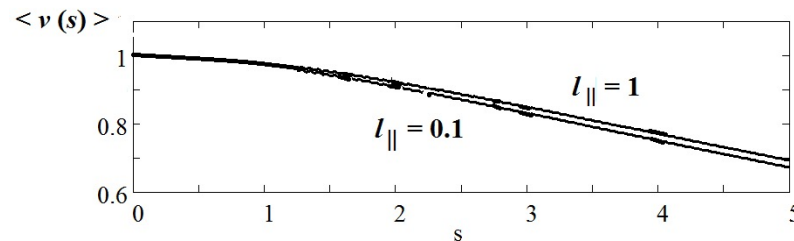


Fig. 2. Attenuation of the mean field of the plane wave at different values of the longitudinal correlation radius of fluctuations. The left panel presents a fragment of the graph on the right panel for the values of the variable s within the range $0 < s < 0.8$. For larger values of s both curves merge.

$$\psi_\varepsilon(s) = \frac{A_\varepsilon(0)}{\pi l_{\parallel}} \frac{(k_0 l_{\parallel})^{\frac{p-2}{2}}}{K_{\frac{p-2}{2}}(k_0 l_{\parallel})} \int_0^\infty \frac{K_{\frac{p-2}{2}}\left(\sqrt{k^2 + (k_0 l_{\parallel})^2}\right)}{\left(\sqrt{k^2 + (k_0 l_{\parallel})^2}\right)^{\frac{p-2}{2}}} \cos \frac{ks}{l_{\parallel}} dk$$



Power spectrum (left) and correlation function (right) in the case of the **inverse power-law** spectrum of fluctuations at several values of inner scale and power exponent ($k_0=0.2$ in these computations).



Computations are performed at $p=3.7$, $k_0=0.5$, $A_\varepsilon(0)=1$.

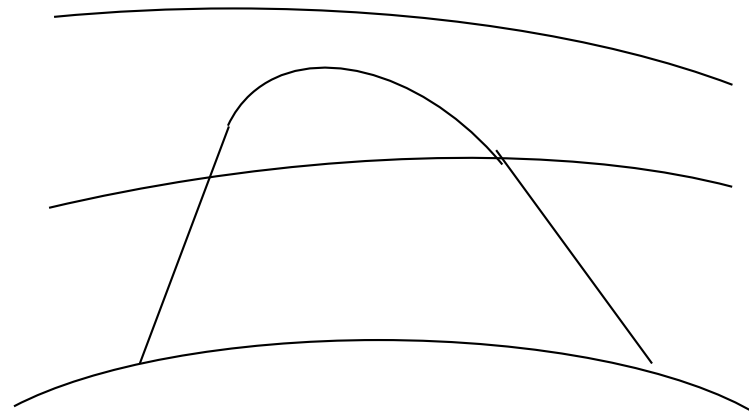
Conclusion

- The analytical technique was developed for calculating the statistical moments of the field in a non-homogeneous background plasma layer, which also contains the fluctuations of the electron density, characterized by a finite value correlation scale.
- The nonlocal equations for the mean field and the coherence function were derived and solved, which presents the next order approximation, as compared to the traditional delta-correlated Markov approximation. It takes account of the finite values of the longitudinal correlation radius of fluctuations of the electron density.
- These results allow for refining the solution for the statistical moments of the field and evaluating the suitability of the first Markov approximation.

IONOSPHERIC REFLECTION CHANNEL

Some problems of modelling the wideband HF ionospheric sky wave channel of propagation will be discussed. The basis for the treatment is the theory of HF propagation in the three-dimensional fluctuating ionosphere. The HF ionospheric fluctuating channel is characterized in terms of the:

- i) statistical moments of the received wideband signals;
- ii) this allows for generating any required random time series of the signal.



One hop path

The basic representation for simulating the pulsed signal propagating through the fluctuating ionosphere is represented as the following Fourier integral

$$E(\mathbf{r}, t, \tau) = \sum_n \int_{-\infty}^{+\infty} P(\omega) T_n(\mathbf{r}, \omega, t) R_n(\mathbf{r}, \omega, t) e^{-i\omega\tau} d\omega \quad (1)$$

\mathbf{E} is the field at the point of observation \mathbf{r} , represented by the sum \mathbf{n} of propagating ionospheric modes;

\mathbf{P} is the spectrum of the launched pulse;

\mathbf{T}_n is the transfer function of the \mathbf{n} -th mode in the background ionosphere;

\mathbf{R}_n are the random functions (also called phasors), which account for the effects of the ionospheric electron density fluctuations on each mode.

t is the slow time describing the quasi stationary motion of the medium

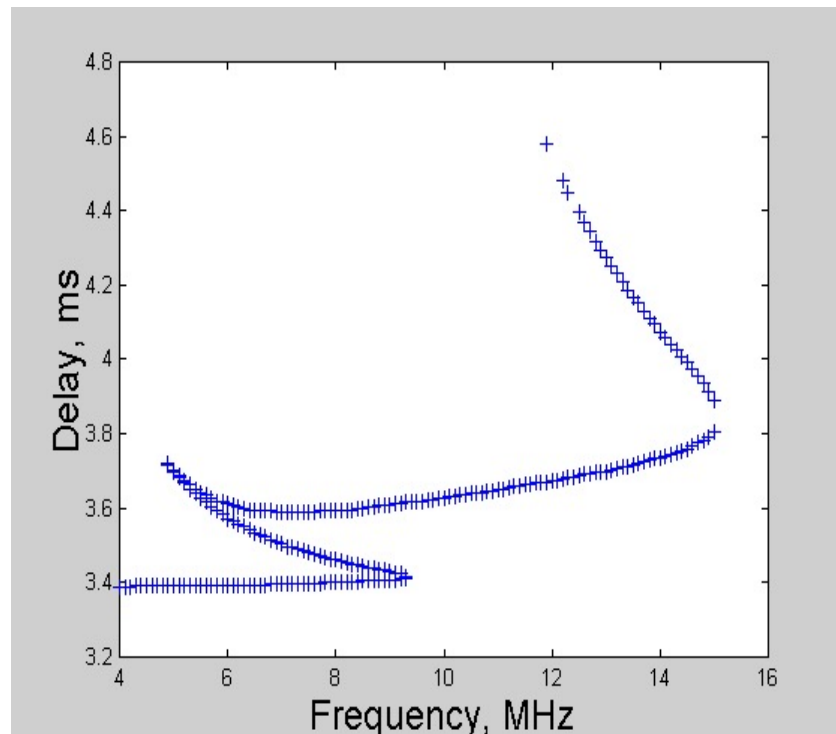
τ is the fast time (fly time) of the signal

Equation (1) is the basic representation, which allows for obtaining the field statistical moments of the signal \mathbf{E} (e.g. scattering function, correlation and coherence functions, etc.), as well as its random time series representation generated.

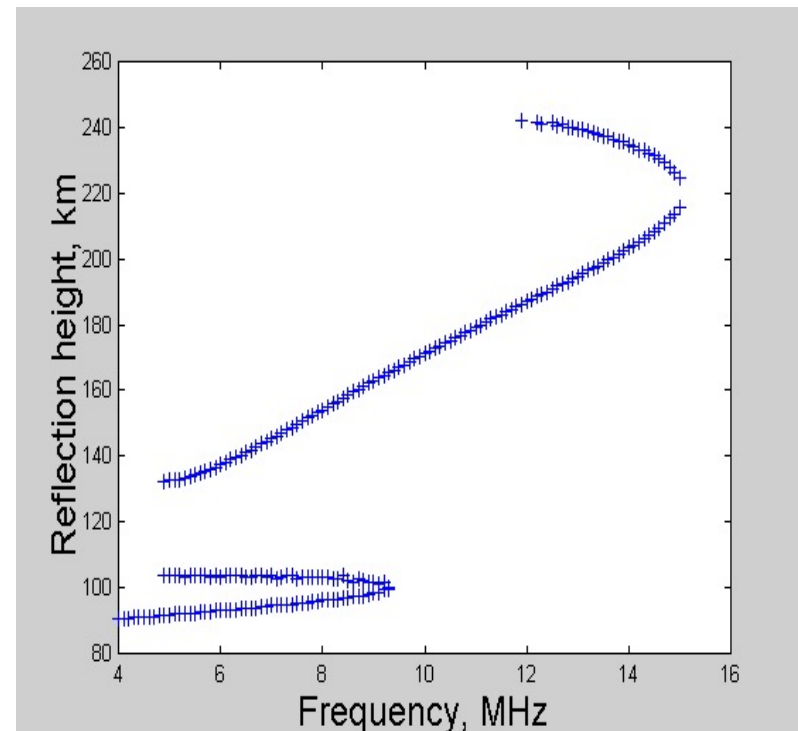
To accomplish this:

- i) transfer functions \mathbf{T}_n of each mode propagating in the background ionosphere should be constructed in terms of the geometrical optics approximation;
- ii) statistical properties of random functions \mathbf{R}_n (phasors) should be described.

Transfer functions T_n is constructed in terms of the geometrical optics employing the ray-tracing technique, so that T_n can be represented for any given model of the background ionosphere.



Left: Ionogram of oblique sounding.



Right: Corresponding reflection height

The random phazors \mathbf{R}_n are represented in terms of complex phases

$$R_n = e^{\psi_n}, \quad \psi_n = \chi_n + iS_n \quad (2)$$

Complex phases are represented by the appropriate integrals, written in ray-centred co-ordinates where ray trajectories constructed for the background ionosphere are employed as the reference rays.

$$\begin{aligned} \psi_1(s_0, 0, 0) = & -\frac{k^2}{4\pi} \iiint ds dq_1 dq_2 \frac{\varepsilon(s, q_1, q_2)}{n_0(s)} h_s(s, q_1, q_2) \left[\det \hat{B}^+(s) \right]^{1/2} \cdot \\ & \exp \left\{ \frac{ik}{2} \left[(b_{11} + b_{11}^g) q_1^2 + (b_{22} + b_{22}^g) q_2^2 + 2(b_{12} + b_{12}^g) q_1 q_2 \right] \right\} \cdot \end{aligned}$$

[2005 (25)] V.E. Gherm, N.N. Zernov, H.J. Strangeways. HF Propagation in a Wideband Ionospheric Fluctuating Reflection Channel: Physically Based Software Simulator of the Channel. *Radio Science*, 40(1), RS1001, doi:10.1029/2004RS003093, 2005.

The scattering effects are described in the Fresnel approximation for forward scattering. As the result, the full-wave type solution of the problem of HF propagation in the fluctuating ionosphere is determined accounting for ray bending and scattering on local random inhomogeneities including the contribution of diffraction in the scattering.

The product of the complex phase method is the spaced time and frequency auto- and cross-correlation functions of S_n and χ_n and their frequency and time spectra.

Correlation functions of complex phases

$$B_{\psi 1}(\omega_1, \omega_2, T_-) = \frac{\pi k_1 k_2}{2} \int_0^{s_0} \frac{ds}{\varepsilon_0(s)} \int d\kappa_n d\kappa_\tau B_\varepsilon(s; 0, \kappa_n, \kappa_\tau) \exp[i\kappa_n(\Delta_n - v_n T_-) + i\kappa_\tau(\Delta_\tau - v_\tau T_-)] \cdot$$

$$\exp\left\{ \frac{i(k_1 - k_2)}{2k_1 k_2} [\kappa_n^2 D_n(s) + \kappa_\tau^2 D_\tau(s) + 2\kappa_n \kappa_\tau D_{n\tau}(s)] \right\},$$

$$B_{\psi 2}(\omega_1, \omega_2, T_-) = - \frac{\pi k_1 k_2}{2} \int_0^{s_0} \frac{ds}{\varepsilon_0(s)} \int d\kappa_n d\kappa_\tau B_\varepsilon(s; 0, \kappa_n, \kappa_\tau) \exp[i\kappa_n(\Delta_n - v_n T_-) + i\kappa_\tau(\Delta_\tau - v_\tau T_-)] \cdot$$

$$\exp\left\{ - \frac{i(k_1 + k_2)}{2k_1 k_2} [\kappa_n^2 D_n(s) + \kappa_\tau^2 D_\tau(s) + 2\kappa_n \kappa_\tau D_{n\tau}(s)] \right\} .$$

This is all further utilised to produce the statistical moments of the full field as well as random time series for S_n , χ_n and the full field.

In the numerical simulation the following anisotropic inverse power law spatial spectrum of fluctuations of the ionospheric electron density is employed

$$B_\varepsilon(\vec{k}, s) = C_N^2 [1 - \varepsilon_0(s)]^2 \sigma_N^2 \left(1 + \frac{K_{tg}^2}{K_{tr}^2} + \frac{\vec{K}_{tr}^2}{K_{tr}^2} \right)^{-p/2}$$

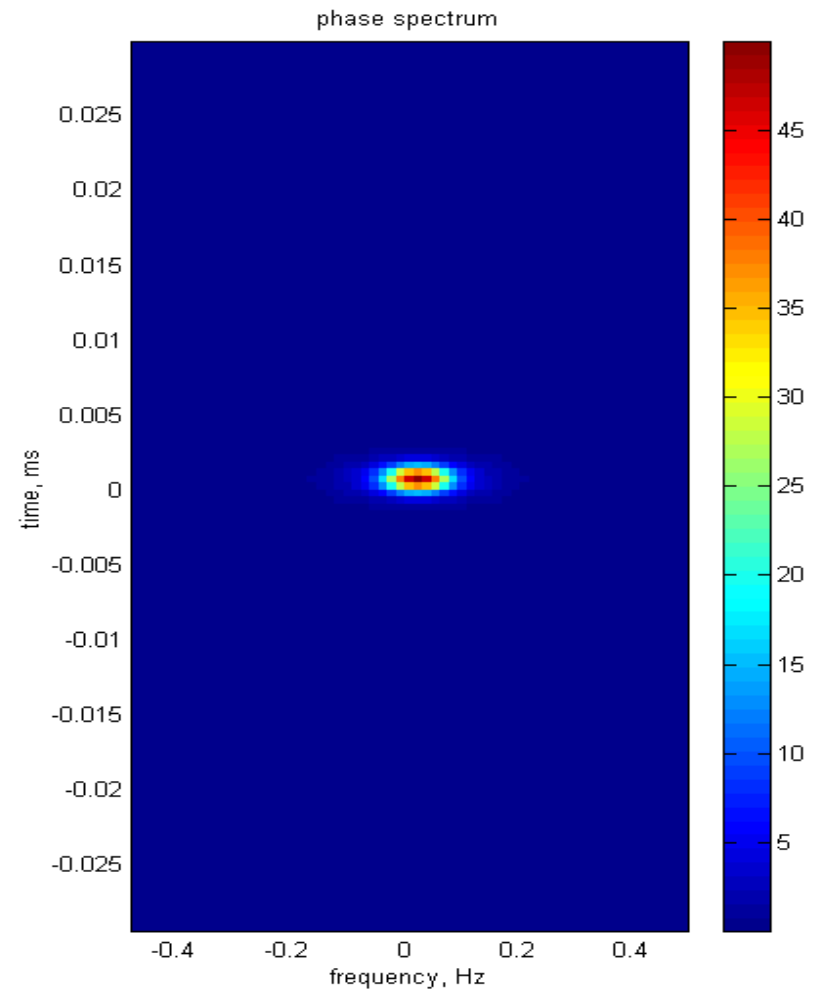
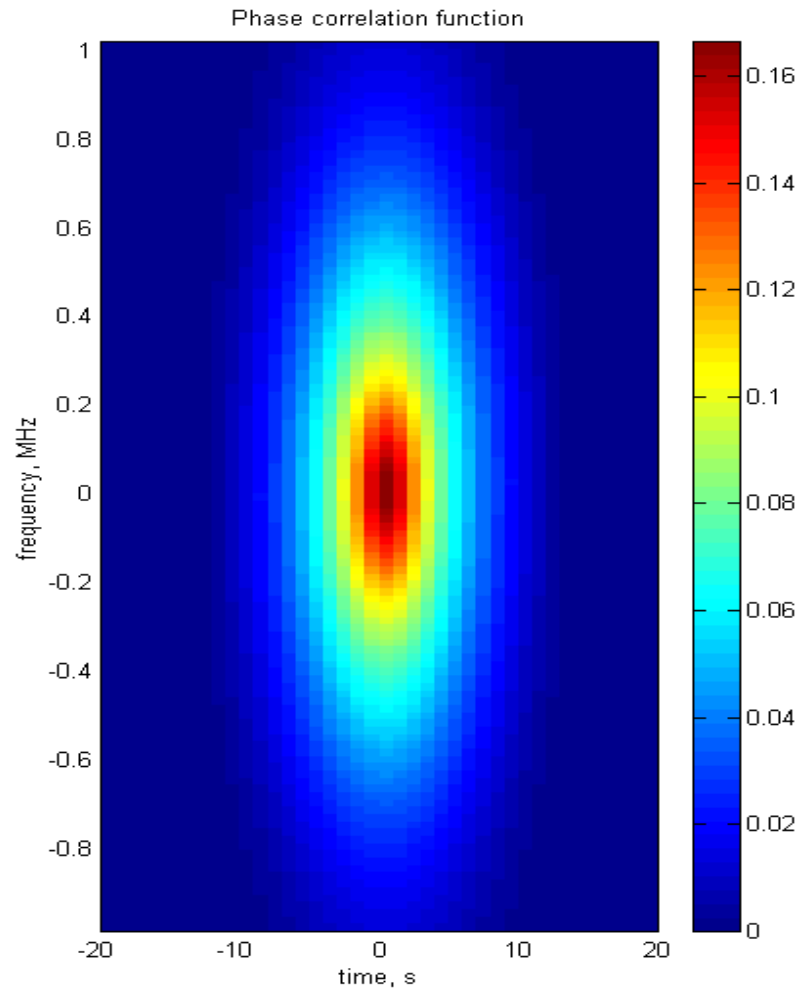
C_N^2 - normalisation coefficient

$\varepsilon_0(s)$ - distribution of the dielectric permittivity of the background ionosphere along the reference ray

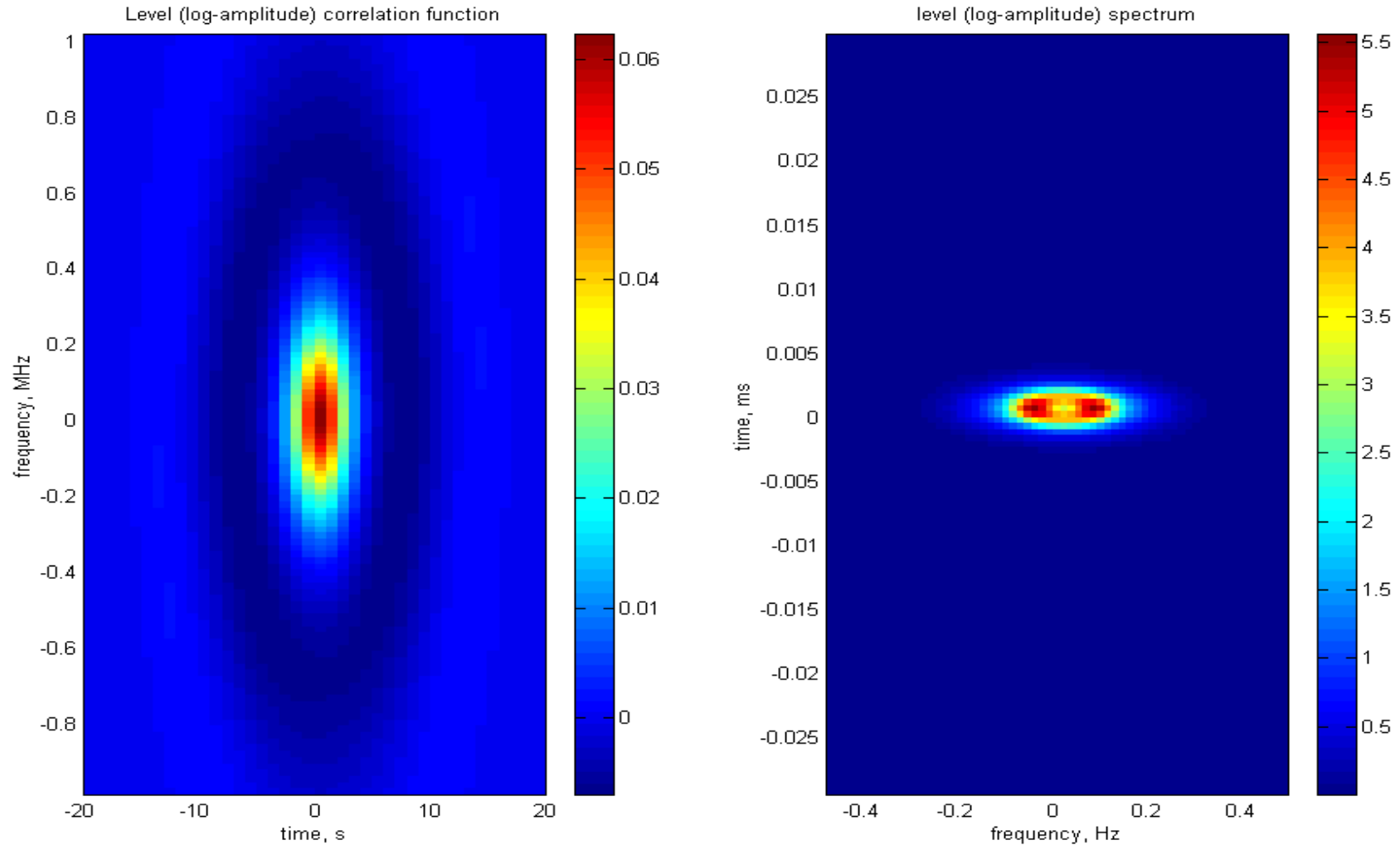
σ_N^2 - variance of the fractional electron density fluctuations

Spaced time and frequency correlation for phase fluctuations and its frequency-time spectrum

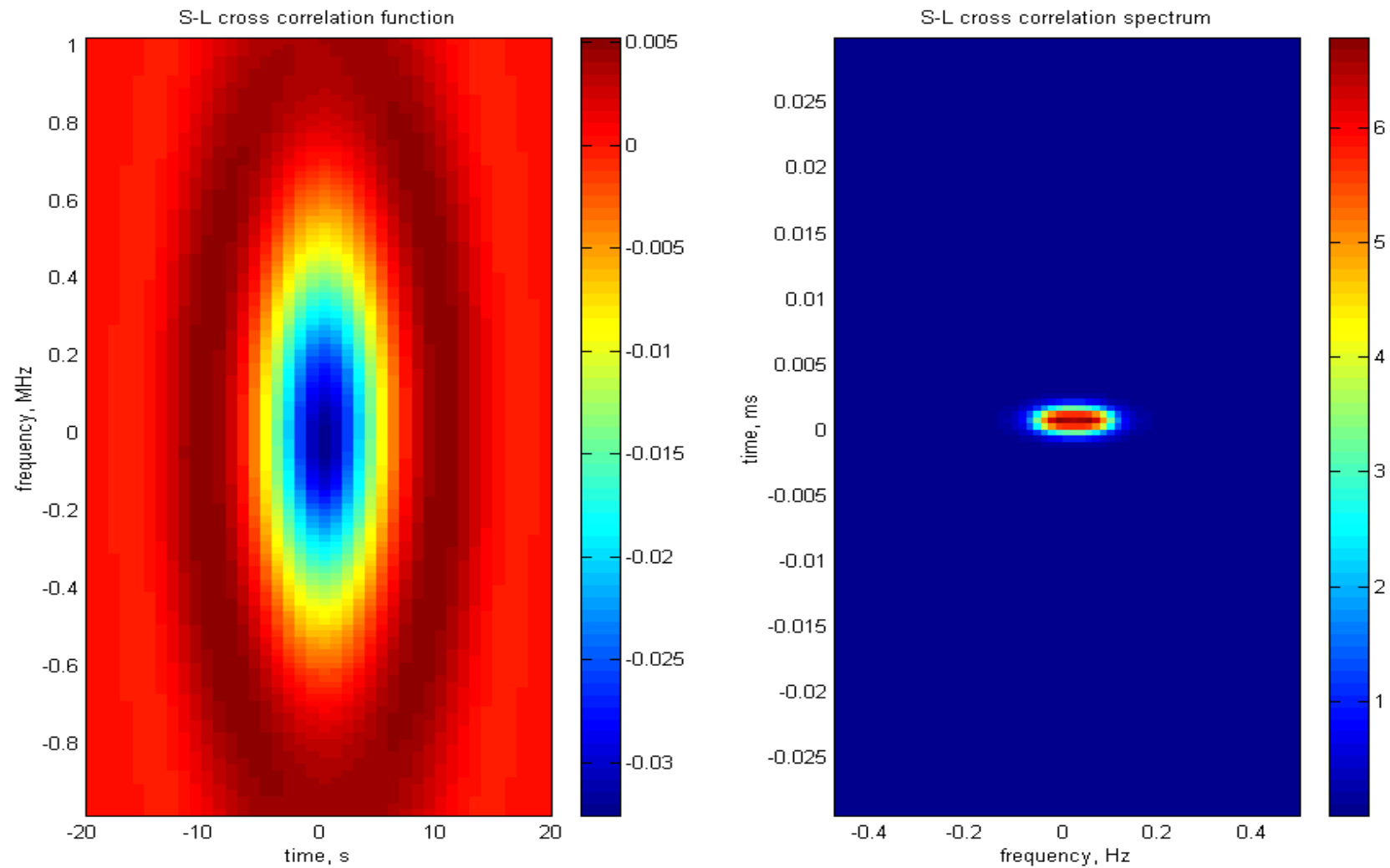
$$S_n$$



Spaced time and frequency correlation for log-amplitude χ_n
and its frequency-time spectrum



Spaced time and frequency cross-correlation function of χ_n and S_n and its frequency-time spectrum



$$E(\mathbf{r}, t, \tau) = \sum_n \int_{-\infty}^{+\infty} P(\omega) T_n(\mathbf{r}, \omega, t) R_n(\mathbf{r}, \omega, t) e^{-i\omega\tau} d\omega \quad (1)$$

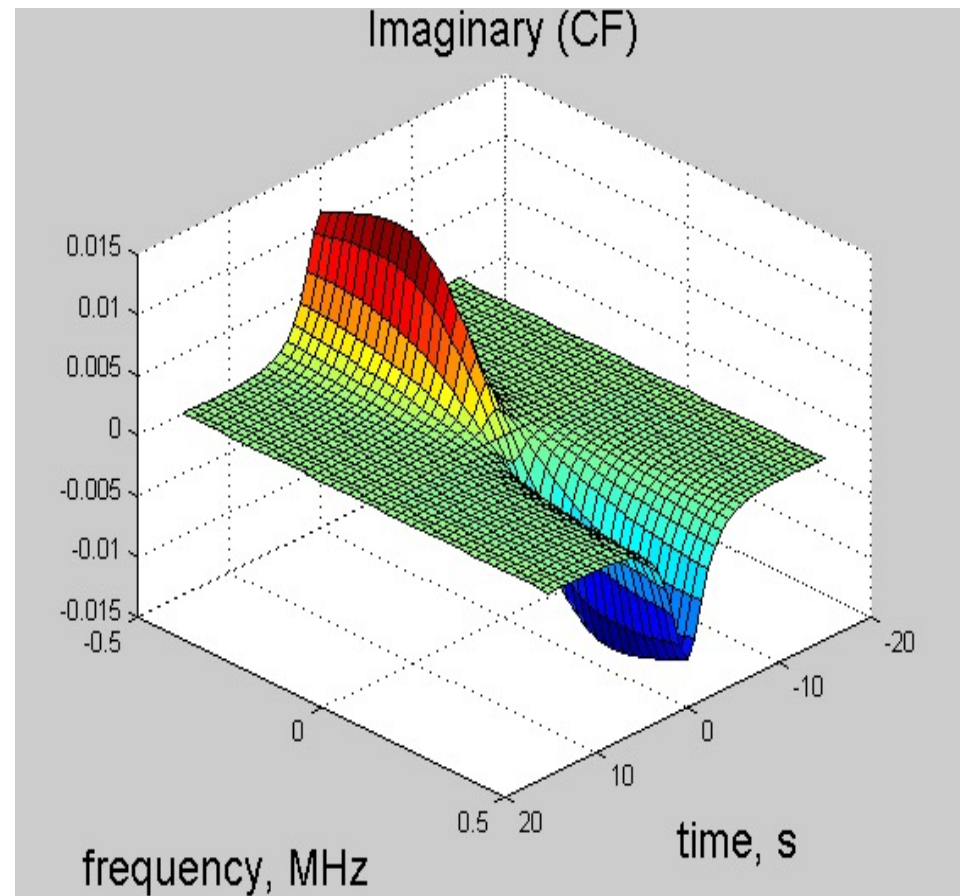
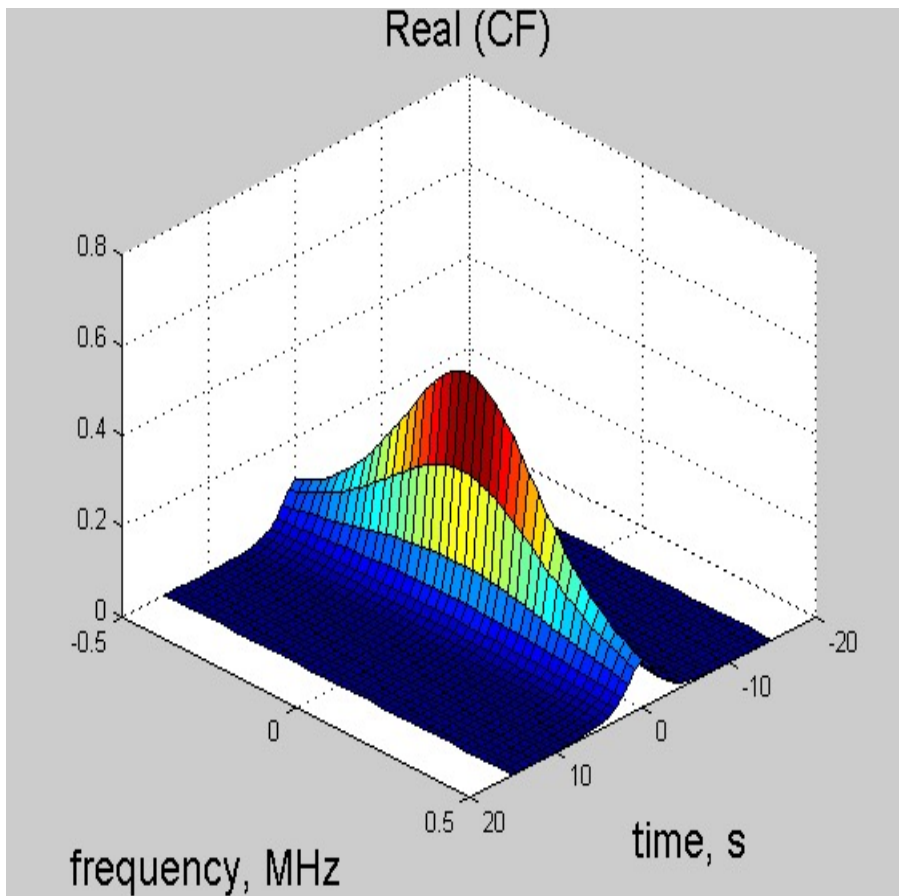
Scattering function for the field E from (1 same as on p.56)

$$F_s(\tau, \omega_d, t) = \frac{1}{2\pi} \iiint P\left(\Omega + \frac{\delta}{2}\right) P^*\left(\Omega - \frac{\delta}{2}\right) \sum_n T_n\left(\Omega + \frac{\delta}{2}, t\right) T_n^*\left(\Omega - \frac{\delta}{2}, t\right)$$

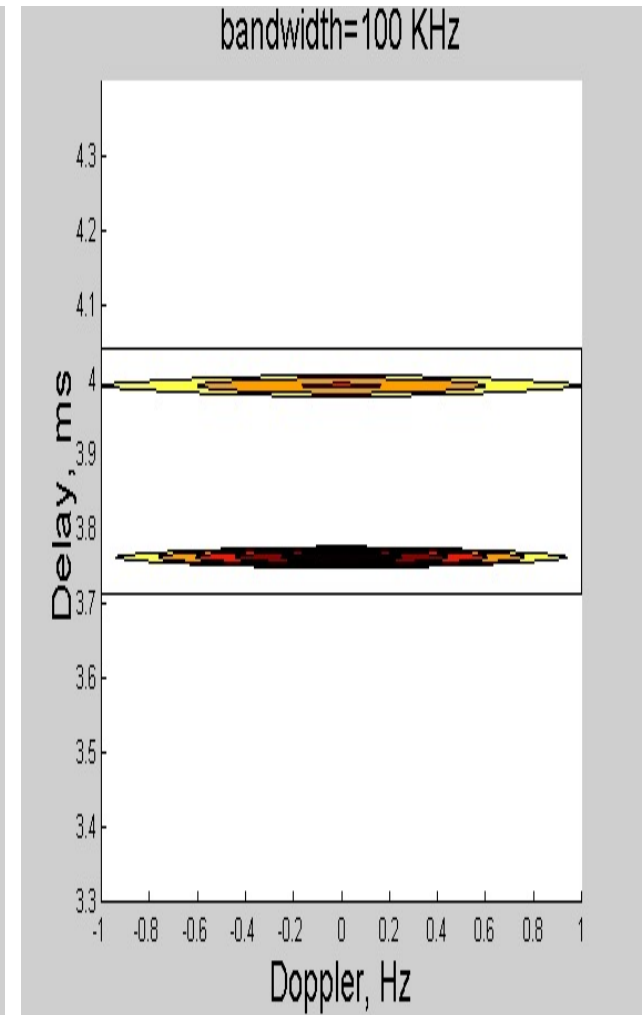
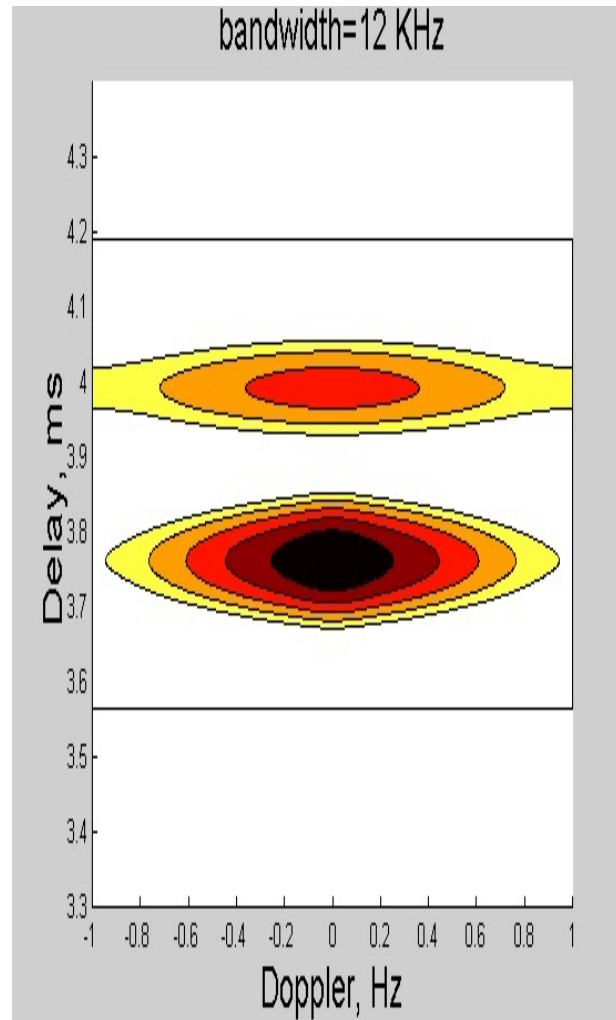
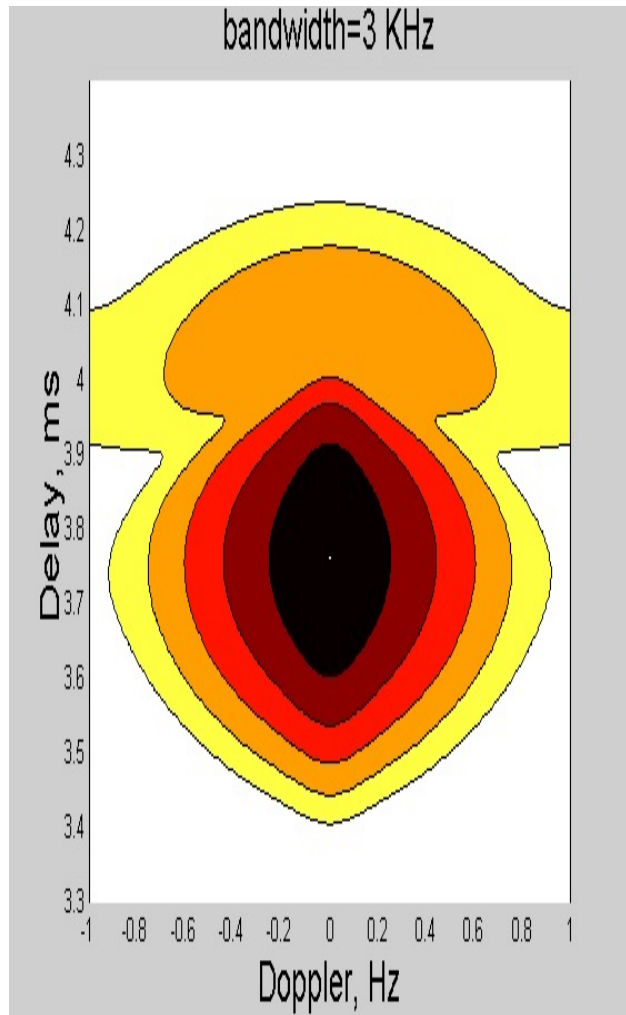
$$\cdot \Psi_n(\Omega, \delta, t, \Delta t) \exp\left\{-i\left[\tau - \tau_{gn}(\Omega)\right]\delta + i\omega_d \Delta t\right\} d\Omega d\delta d\Delta t$$

$\Psi_n(\Omega, \delta, t, \Delta t)$ is the correlation function for R_n expressed in terms of correlation functions of \mathcal{X}_n and S_n .

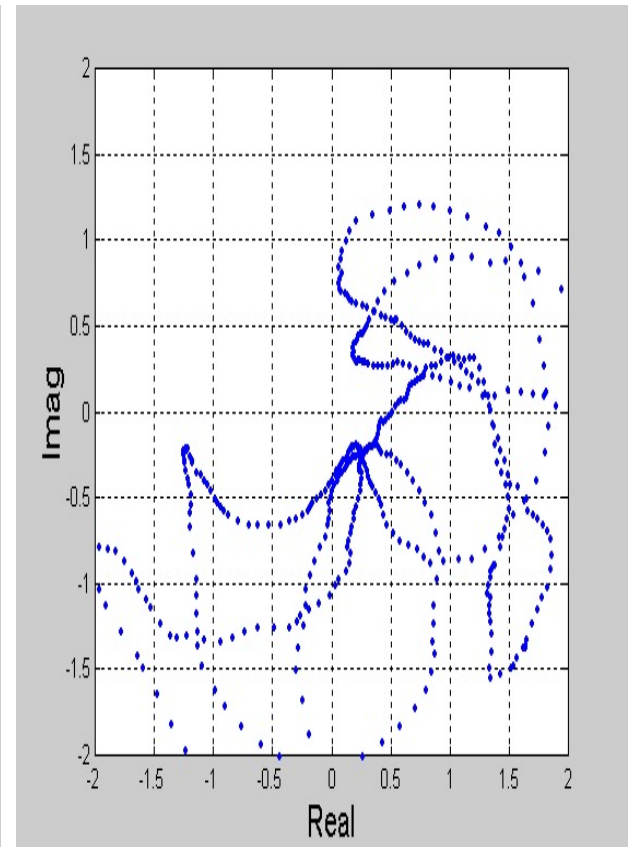
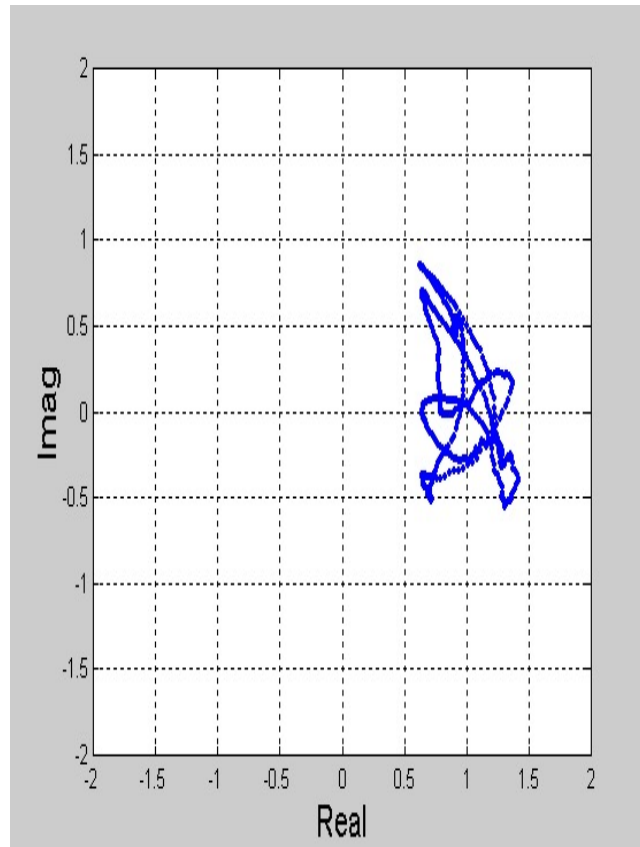
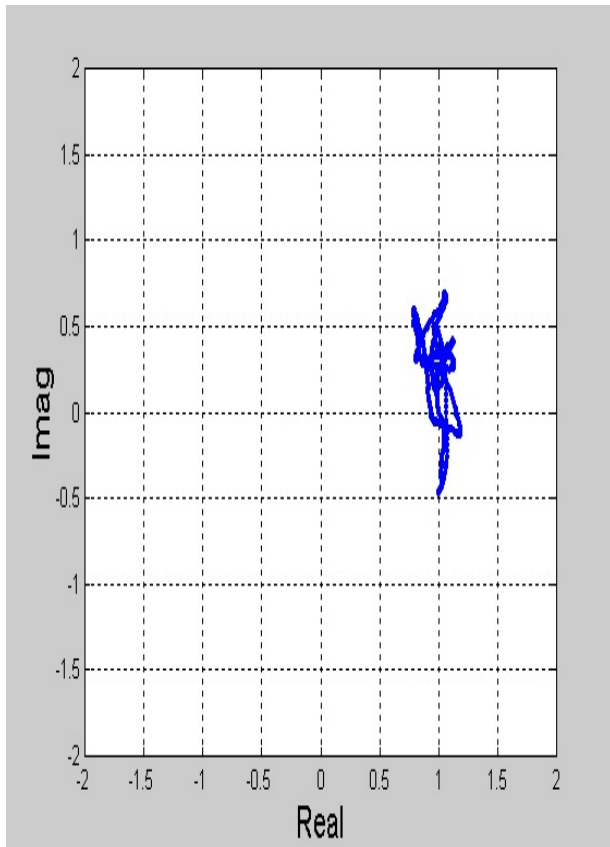
Spaced time and frequency correlation function $\Psi_n(\Omega, \delta, t, \Delta t)$ of the random phasor R_n (for the fixed value of Ω)



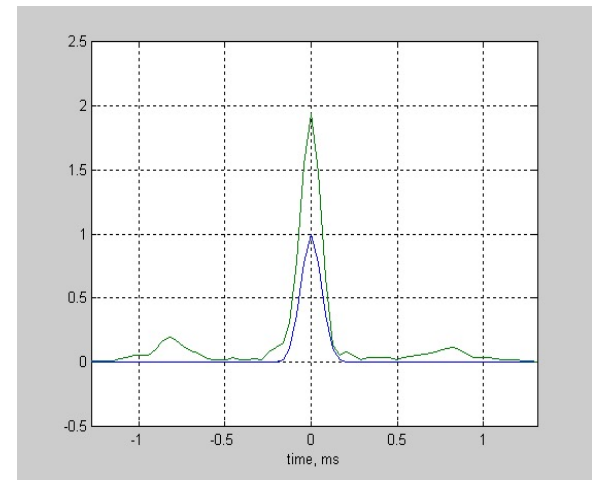
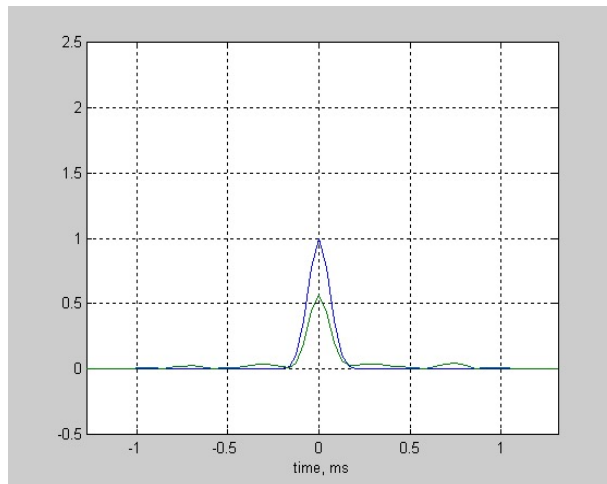
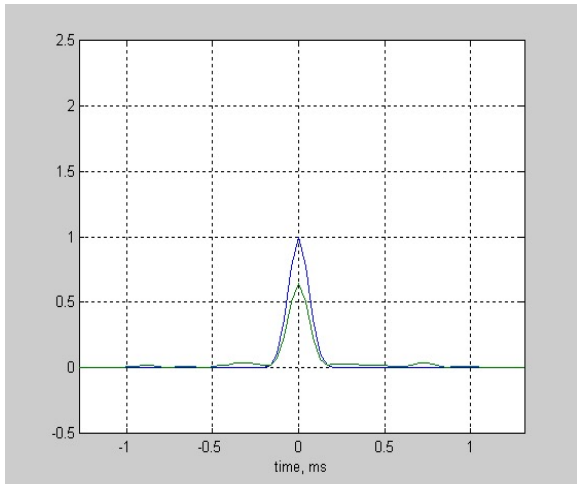
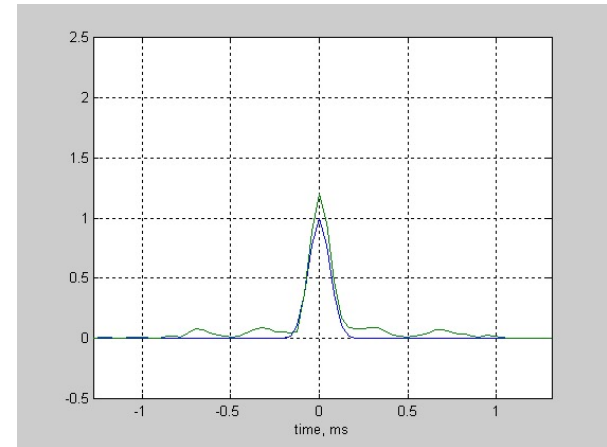
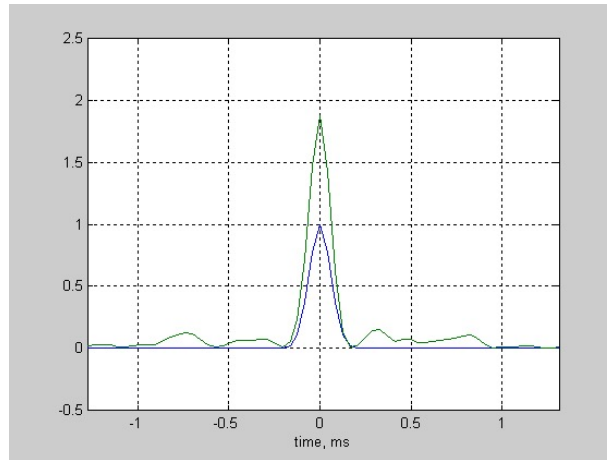
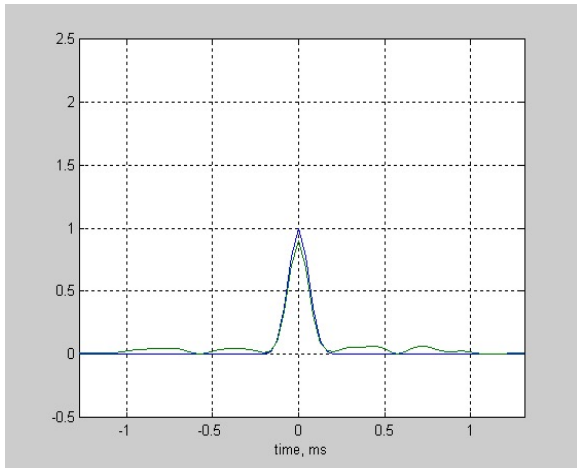
Two-mode scattering function



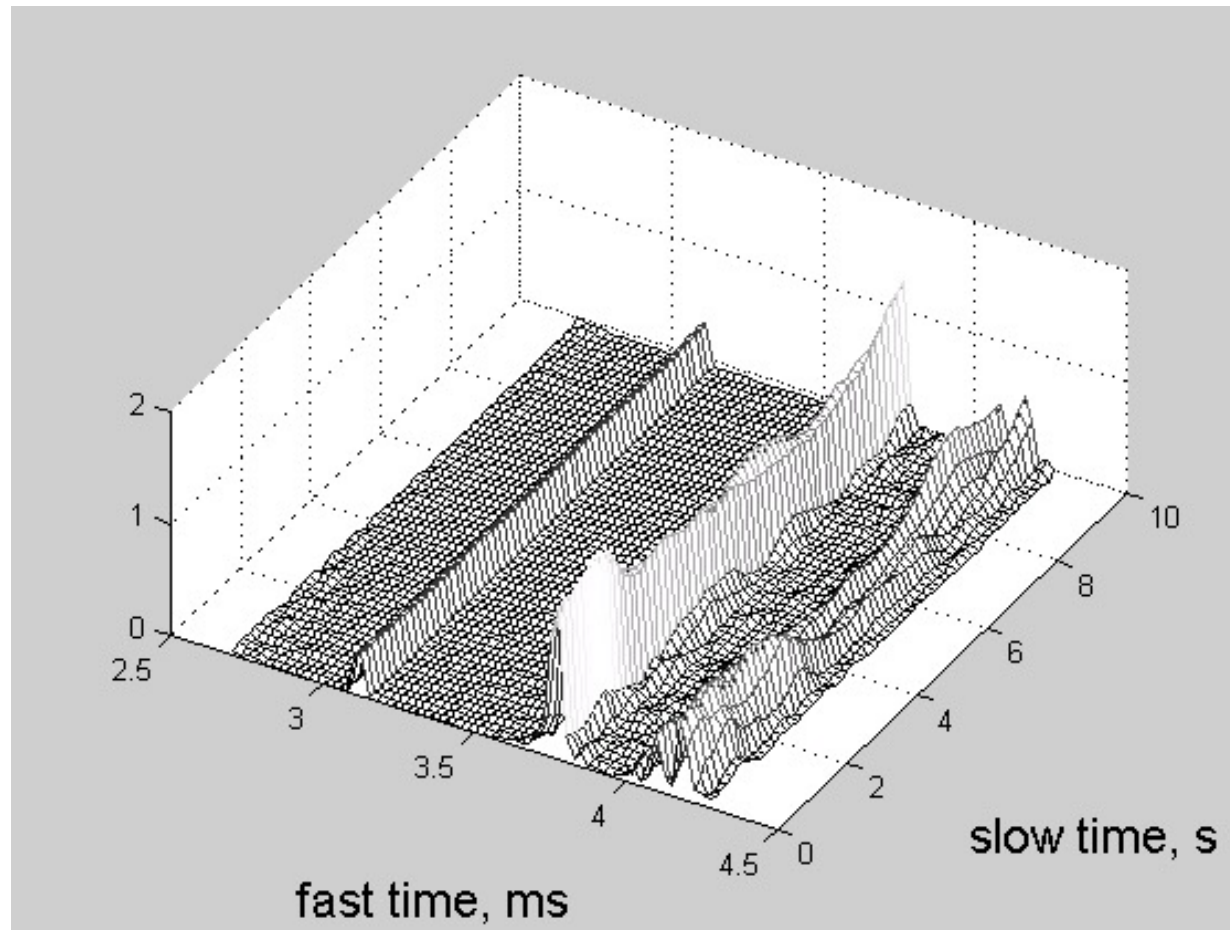
Time random walk of R_n for a given frequency



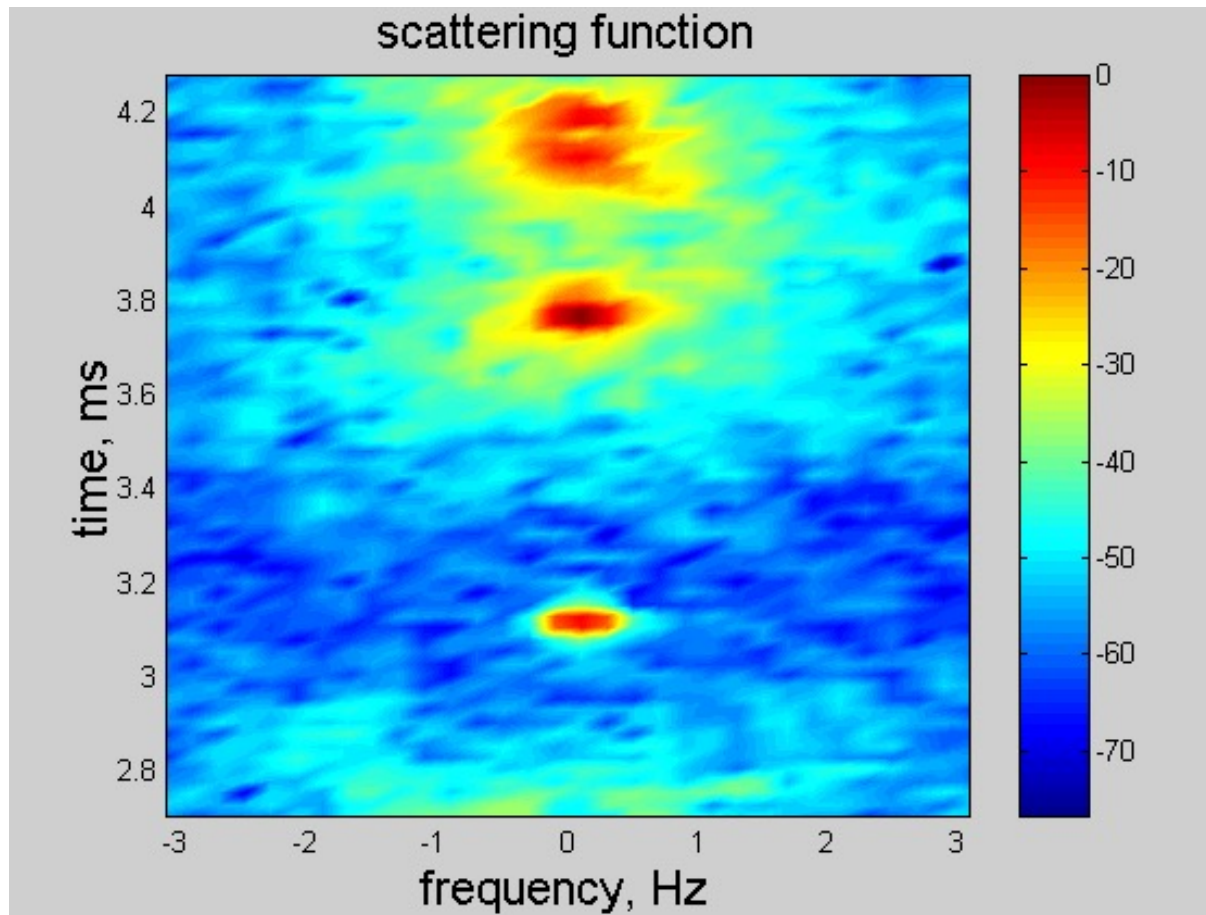
Impulse with the bandwidth 12 kHz



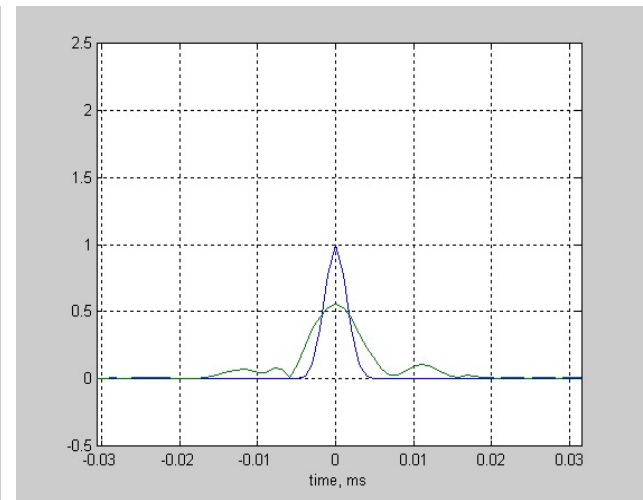
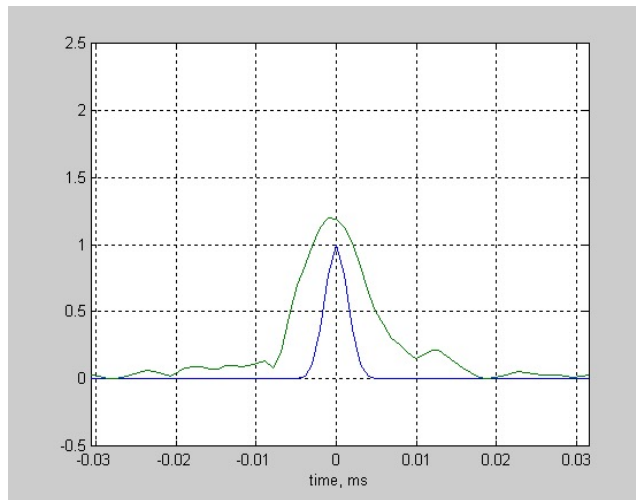
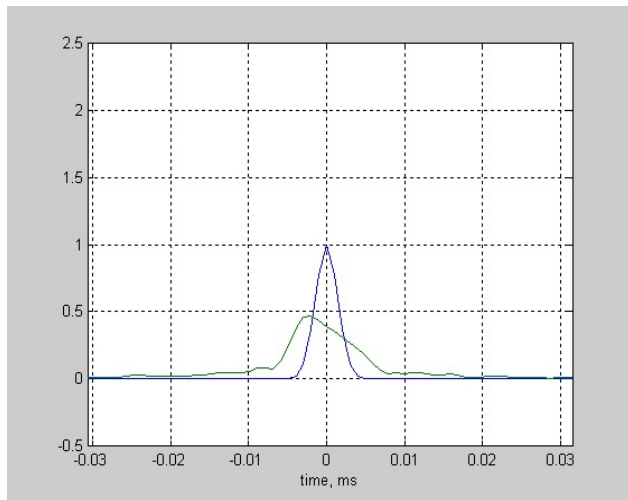
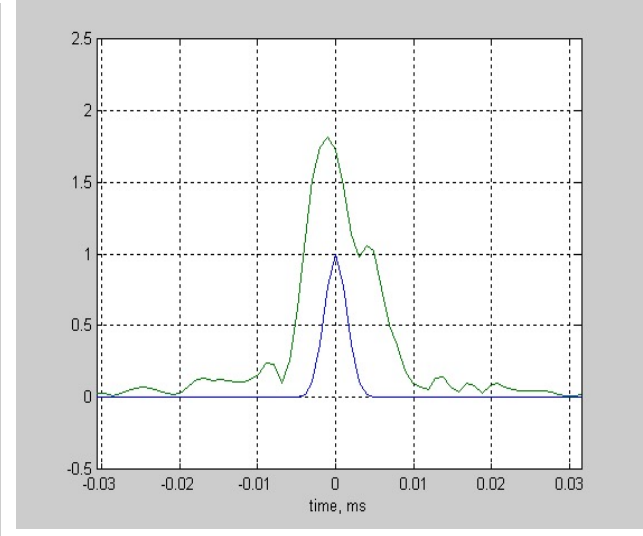
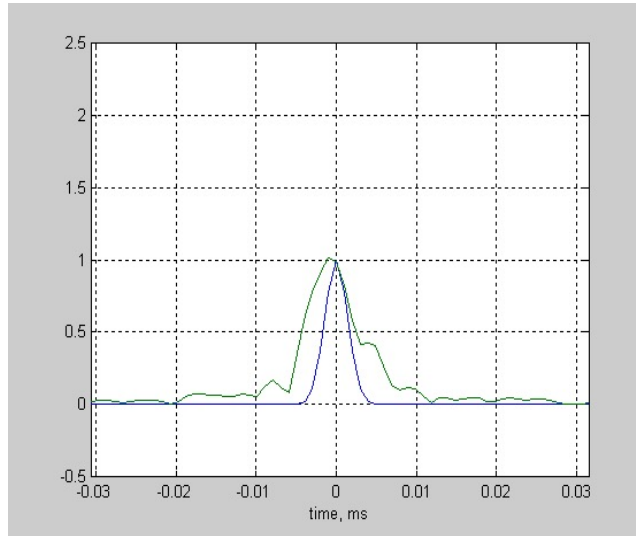
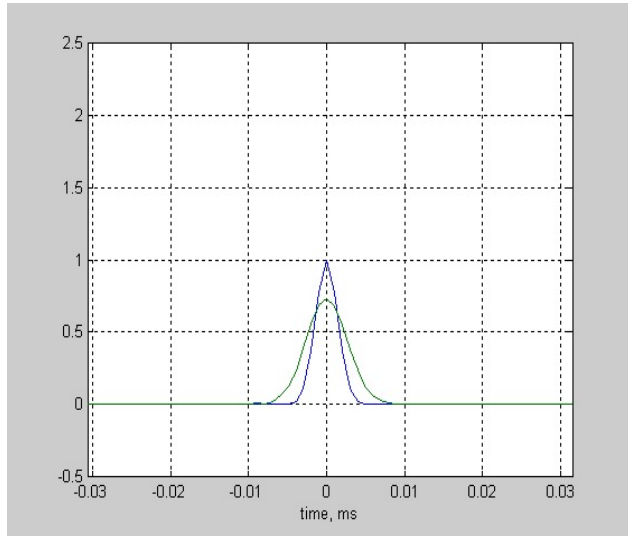
Simulated realizations of the multi-moded pulse propagation.
The pulse length is $25\ \mu\text{s}$.



Scattering function reconstructed from the simulated realizations of the pulse propagation. The pulse length is 25 μs .



Impulse with the bandwidth 500 KHz



As the result:

The analytic-numerical technique demonstrated allows simulation of the effects on the wideband ionospheric HF channels of a wide range of the following parameters:

- (1) the transmission bandwidth
- (2) the transmission frequency
- (3) the variance of fractional electron density fluctuations
- (4) the speed and direction of the drift of the turbulence
- (5) the anisotropy and outer scale of the irregularities
- (6) the background ionosphere model
- (7) the orientation of the propagation path to the geomagnetic meridian
- (8) the multi-mode effects.

Final remarks:

We have presented here the complete description of the transionospheric stochastic channel of propagation. This included both the cases of weak and strong scintillation of the fields of the frequencies of 100 – 1000 MHz.

As far as the ionospheric reflection HF channel is concerned, its description was confined by the case of weak fluctuations (scintillation). This is because at frequencies of the HF band the diffraction effects of the field on local random inhomogeneities of the ionospheric electron density are much more pronounced, than for the band of 100 – 1000 MHz.

Taking these effects into account for frequencies of the HF band requires further extension of the known theories. The extended theory should be able to describe the essential diffraction effects of the field on local random inhomogeneities of the electron density of the ionosphere in the conditions of fairly inhomogeneous background ionosphere, which additionally gives birth to essentially curved ray paths in the background ionosphere. This is the subject for further investigation.